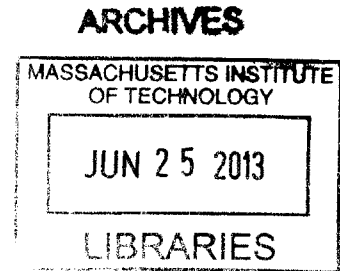


Translation of Dilution Tolerance for Gasoline SI Engine

by

Troy S. Niekamp

B.S. Mechanical Engineering  
Ohio State University, 2011



SUBMITTED TO THE DEPARTMENT OF MECHANICAL ENGINEERING  
IN PARTIAL FULLFILMENT OF THE REQUIREMENTS FOR THE DEGREE OF

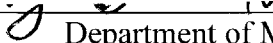
MASTER OF SCIENCE IN MECHANICAL ENGINEERING  
AT THE  
MASSACHUSETTS INSTITUTE OF TECHNOLOGY

JUNE 2013

© 2013 Massachusetts Institute of Technology  
All Rights Reserved

The author hereby grants to MIT permission to reproduce  
and to distribute publicly paper and electronic  
copies of this thesis document in whole or in part  
in any medium now known or hereafter created.

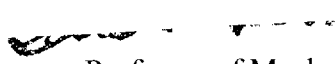
Signature of Author:

\_\_\_\_\_   
Department of Mechanical Engineering  
May 10, 2013

Certified by:

\_\_\_\_\_   
Wai K. Cheng  
Professor of Mechanical Engineering  
Thesis Supervisor

Accepted by:

\_\_\_\_\_   
David E. Hardt  
Professor of Mechanical Engineering  
Chairman, Committee for Graduate Students



# **Translation of dilution tolerance for Gasoline SI Engine**

by

Troy Niekamp

Submitted to the Department of Mechanical Engineering  
on May 10, 2013 in Partial Fulfillment of the  
Requirement for the Degree of Masters of Science in  
Mechanical Engineering

## **ABSTRACT**

There are a variety of fuel improvement strategies being developed for spark ignition engines which use dilution. Many of these technologies use a combination of different diluents. It is impractical in optimizing these technologies to test every possible combination of diluents. The purpose of this study was to determine a relationship between the various diluents and combustion related output parameters. One of these key outputs was determining the dilution tolerance for an engine. In order to achieve this goal, the fundamental of combustion were studied.

The results from this study will be useful in developing more aggressive engine control strategies. Dilution has been studied extensively in previous research. Its effects are well known. Primarily, it reduces peak combustion temperatures. This can be used as an effective means to reduce losses and hazardous emissions. Too much dilution, however, and the combustion stability is compromised.

To facilitate this project, an engine was fully instrumented. Experiments were performed for a variety of operating conditions and diluents. Results were then used to correlate the diluent properties and quantities to combustion outputs. Adiabatic flame temperature was first attempted as the key metric for correlation. This metric proved to be unsuitable for developing correlations. Later, a new metric was computed by taking a linear combination of diluents. This was found to offer superior results. Using this metric along with other basic engine measurements, correlations were developed between the diluents and engine output parameters. These output parameters include dilution tolerance, exhaust temperature, NO<sub>x</sub> emissions, and combustion burn durations.

**Thesis Supervisor:** Wai K. Cheng

**Title:** Professor of Mechanical Engineering



## ACKNOWLEDGMENTS

There are a variety of people that without them my research would have not been possible. Certainly I cannot acknowledge everyone, but I will mention those that played key roles in my research experience at MIT.

First of all, I would like to thank Professor Wai Cheng in imparting upon me the knowledge and intellect need to perform engine research. His leadership and guidance were vital in achieving results and troubleshooting when problems occurred.

Next, I would like to thank the personnel at Sloan Auto Laboratory. This includes Janet Maslow for ensuring that all administrative matters were handled smoothly; Thane Dewitt for assisting with my engine setup; and Raymond Phan for constructing any apparatus I needed. My research would have taken twice as long without him.

Furthermore, there were some outstanding graduate students at the Sloan Automotive Laboratory who assisted my engine research and provided general guidance during my stay at MIT. Specifically, Ph.D. student Kevin Cedrone was a tremendous help in regards to my engine and data acquisition setup. Many thanks also to Tomas Vianna for his hands-on engine experience and Amelia Brooks for UROP help. Finally, Chris James, Mike Plumley, Mark Molewyk Mol, and Sang Wen for being great officemates and friends.

Of course this research could not have been possible without my sponsors at The Ford Motor Company. Their insight and guidance throughout my project was much appreciated. I would like to mention Gopi Surnilla specifically for being a sharp project lead and with an optimistic attitude.

Finally, I would like to thank my friends and family for their support during my graduate stay at The Massachusetts Institute of Technology. It was great knowing that someone always had my back and was there for me through my struggles.



# TABLE OF CONTENTS

ABSTRACT.....	3
ACKNOWLEDGMENTS .....	5
TABLE OF CONTENTS.....	7
LIST OF FIGURES .....	10
LIST OF TABLES.....	12
NOMENCLATURE .....	13
CHAPTER 1 – INTRODUCTION .....	15
1.1 Background .....	15
1.2 Control Strategy & Dilution.....	17
1.2.1 EGR .....	18
1.2.2 Lean Combustion.....	20
1.2.3 Water Vapor Compensation .....	21
1.3 Dilution Tolerance.....	23
1.4 Research Objectives .....	25
1.4.1 Choosing a lumped metric.....	26
1.5 Adiabatic Flame Temperature.....	26
CHAPTER 2 – EXPERIMENTAL METHODS .....	30
2.1 Test Engine Setup.....	30
2.1.1 Dynamometer .....	30
2.1.2 Injection/Ignition Control.....	31
2.1.3 Air & Fuel Control / Measurement.....	32
2.1.4 EGR Loop and CO <sub>2</sub> Measurement .....	33

2.1.5 Water Vapor Injection .....	34
2.1.6 Cylinder Pressure Measurement.....	35
2.1.7 Temperature Measurement.....	36
2.1.8 NOx Measurement.....	36
2.1.9 Fuel .....	37
2.2 Data Acquisition.....	37
2.3 Testing Methodology .....	38
2.3.1 Engine Experiments.....	38
2.3.2 Combustion Phasing.....	40
CHAPTER 3 – EXPERIMENTAL DATA ANALYSIS .....	41
3.1 NIMEP .....	41
3.2 CoV of NIMEP.....	42
3.3 Heat Release Profiles .....	43
3.4 Specific NOx .....	43
3.5 EGR Determination.....	44
3.6 NISFC.....	45
CHAPTER 4 – GTP MODELING .....	46
4.1 GT-Power Overview .....	46
4.2 Model Matrices: .....	48
4.3 Model Results.....	49
CHAPTER 5 – Results.....	51
5.1 Adiabatic Flame Temperature.....	51
5.1.1 Trapped Charge Composition.....	51
5.1.2 Reference Condition .....	52
5.1.3 Calculation Method .....	53



5.1.4 Correlation Plots .....	54
5.2 Ford EGR-Intake-Equivalent .....	57
5.2.1 Humidity + EGR Equivalent .....	57
5.2.2 Lean + EGR Equivalent.....	57
5.2.3 Overall Equivalent .....	58
5.2.3 Correlation Plots .....	59
5.3 Regression of Diluents .....	61
5.3.1 Methodology.....	61
5.3.2 Correlation Plots .....	62
5.4 Interaction Effects .....	65
CHAPTER 6 – CONCLUSIONS .....	67
REFERENCES .....	69
APPENDIX A.....	71
Standard Operating Procedure .....	71
APPENDIX B.....	74
Fuel Specifications .....	74
Appendix C .....	76
Interaction Plots.....	76

## LIST OF FIGURES

Figure 1: Trends in attributes of new cars, 1975-2005 .....	15
Figure 2: US Emissions Regulation (AGCO, 2013).....	16
Figure 3: NOx formation rate (AlenTecinc.com) .....	17
Figure 4: Schematic of EGR loop (Novinky, 2010) .....	18
Figure 5: Pumping Loop (Mechadyne International 2012) .....	20
Figure 6: Variation of exhaust NO concentration with A/F and fuel/air equivalence ratio. Spark-ignition engine, 1600 rev/min, $\eta_v = 50$ percent. (Heywood 1988).....	21
Figure 7: Atmospheric dewpoints versus temperature (Benson 2004).....	22
Figure 8: United States Humidity Zones (Tabor 2001) .....	22
Figure 9: CoV and lambda.....	24
Figure 10: CoV for EGR and lambda sweeps.....	25
Figure 11: Adiabatic Flame Temperature, Isooctane (Depcik 2013) .....	27
Figure 12: Burning velocity vs flame temperature; Propane, $T_{unb} = 563$ K, $P = 1.22$ bar (Pischinger 1985).....	29
Figure 13: Engine/Dyno setup .....	31
Figure 14: Fuel injector calibration for test engine.....	32
Figure 15: CO <sub>2</sub> Measurement .....	34
Figure 16: Water Injector Calibration.....	35
Figure 17: Pressure Transducer Calibration .....	36
Figure 18: LabVIEW screenshot .....	37
Figure 19: Pressure trace at part load.....	41
Figure 20: Sample Histogram of NIMEP .....	42
Figure 21: MFB and Qapp trace for test at part load .....	43
Figure 22: EGR vs CO <sub>2</sub> .....	45
Figure 23: GT-Power Model.....	47
Figure 24: Residual gas composition – EGR sweep.....	49
Figure 25: Residual gas composition – lambda sweep .....	49
Figure 26: Residual gas composition – water vapor sweep.....	50
Figure 27: Adiabatic Flame Temperature comparison at 1500 rpm, 3.6 bar NIMEP .....	53
Figure 28: Polynomial Coefficients (Heywood 1988).....	54

Figure 29: T-adiab correlations, Condition 1 .....	54
Figure 30: T-adiab correlations, Condition 2 .....	55
Figure 31: T-adiab correlations, Condition 3 .....	55
Figure 32: EGR equivalent correlations, Condition 1 .....	59
Figure 33: EGR equivalent correlations, Condition 2 .....	59
Figure 34: EGR equivalent correlations, Condition 3 .....	60
Figure 35: Linear combination equivalent correlations, Condition 1 .....	62
Figure 36: Linear combination equivalent correlations, Condition 2 .....	63
Figure 37: Linear combination equivalent correlations, Condition 3 .....	63
Figure 38: EGR – H <sub>2</sub> O interaction plot.....	65
Figure 39: H <sub>2</sub> O – Lean.....	66
Figure 40: H <sub>2</sub> O – Lean Interaction, Condition 1.....	76
Figure 41: H <sub>2</sub> O – Lean Interaction, Condition 2.....	76
Figure 42: H <sub>2</sub> O – Lean Interaction, Condition 3.....	77
Figure 43: EGR – Lean Interaction, Condition 1.....	77
Figure 44: EGR – Lean Interaction, Condition 2.....	78
Figure 45: EGR – Lean Interaction, Condition 3.....	78
Figure 46: EGR – H <sub>2</sub> O Interaction, Condition 1.....	79
Figure 47: EGR – H <sub>2</sub> O Interaction, Condition 2.....	79
Figure 48: EGR – H <sub>2</sub> O Interaction, Condition 3.....	80

## LIST OF TABLES

Table 1: Test Engine Specs.....	30
Table 2: Thermocouple locations.....	36
Table 3: Measurement Channels.....	38
Table 4: Single diluent tests.....	39
Table 5: Test Matrix, EGR + Lean .....	39
Table 6: Test Matrix, EGR + Lean .....	39
Table 7: Test Matrix, EGR + Water Vapor.....	39
Table 8: Single diluent simulation .....	48
Table 9: EGR+ H <sub>2</sub> O simulation .....	48
Table 10: EGR+ $\lambda$ simulation .....	48
Table 11: $\lambda$ + H <sub>2</sub> O simulation .....	48
Table 12: Linear combination coefficients .....	62

## NOMENCLATURE

AFR	Air Fuel Ratio
ATDC	After Top Dead Center
BDC	Bottom Dead Center
BTDC	Before Top Dead Center
CA	Crank Angle
CAD	Crank Angle Degrees
CA50	50% MFB point
CoV	Coefficient of Variation
EGR	Exhaust Gas Recirculation
EVC	Exhaust Valve Close
EVO	Exhaust Valve Open
DI	Direct Injection
IVC	Intake Valve Close
IVO	Intake Valve Close
MAP	Manifold Absolute Pressure
MBT	Maximum Brake Torque
MFB	Mass Fraction Burned
MY	Model Year
NIMEP	Net Indicated Mean Effective Pressure
NISFC	Net Indicated Specific Fuel Consumption
NO <sub>x</sub>	Nitric Oxides
PFI	Port Fuel Injection
PM	Particulate Matter
RPM	Revolutions per Second
SI	Spark Ignition
S <sub>L</sub>	Flame Speed
SOI	Start of Injection
TDC	Top Dead Center
$c_v$	Specific heat capacity at constant volume

$c_p$	Specific heat capacity at constant pressure
$m$	Mass
$\dot{m}$	Mass flow rate
$n$	Hydrogen to carbon ratio of fuel, i.e. CH.
$n_a$	Moles of air
$n_f$	Moles of fuel
$p$	Pressure
$T$	Temperature
$W$	Molecular weight
$X$	Mole fraction
$\lambda$	Lambda, normalized AFR
$\phi$	Phi, fuel air equivalence ratio
$\rho$	Density
$\theta$	Theta, crank angle degrees
$\mathfrak{R}$	Universal gas constant
$\gamma$	specific heat ratio, $c_p/c_v$
$sp$	instantaneous piston speed normalized by mean

# CHAPTER 1 – INTRODUCTION

## 1.1 Background

Tightening of emissions requirements in the United States and Europe brings about the need to develop new technologies just to maintain current automotive performance. On top of this, consumers constantly seek increased horsepower, better acceleration, more safety features, and better fuel economy. Figure 1 depicts basic trends over the years. (Feng 2007). These competing forces create the need for new advanced technology and the refinement of existing technologies. Many opportunities are being explored by automotive, lubricant, and energy companies to meet these consumer needs while also complying with stringent emissions regulations.

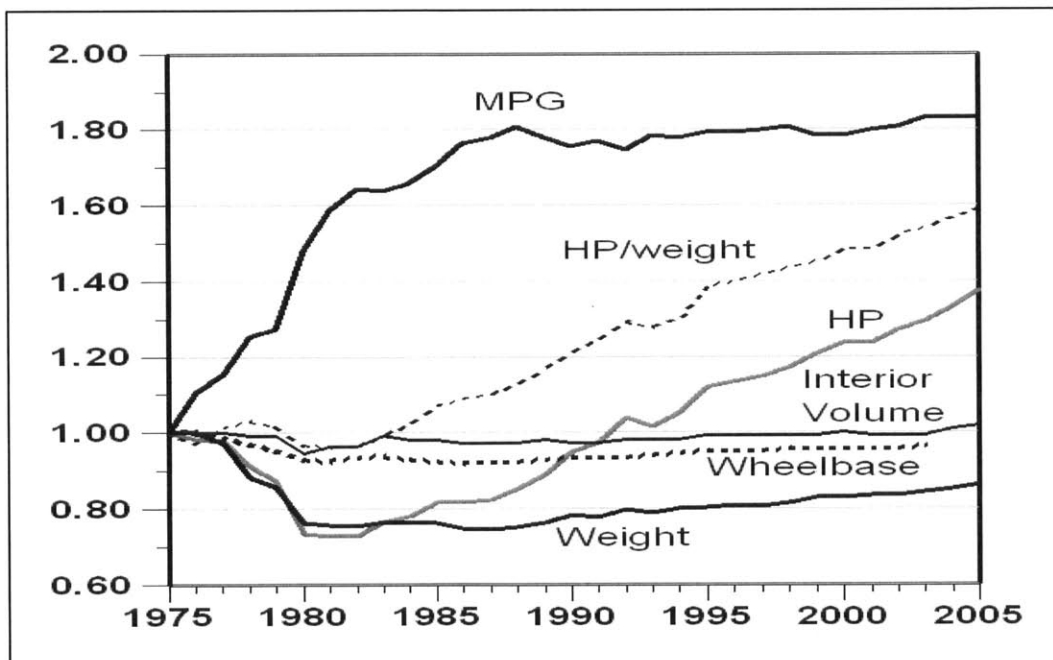


Figure 1: Trends in attributes of new cars, 1975-2005

These stringent emissions regulations make it much more difficult for automakers to advance efficiency. Figure 2 shows the history of the allowable nitric oxide (NOx) emissions versus the allowable particulate matter (PM) emissions in the United States. An exponential reduction in allowable emissions can be observed. The emissions requirements set for 2014 are a small fraction of what they were in previous years

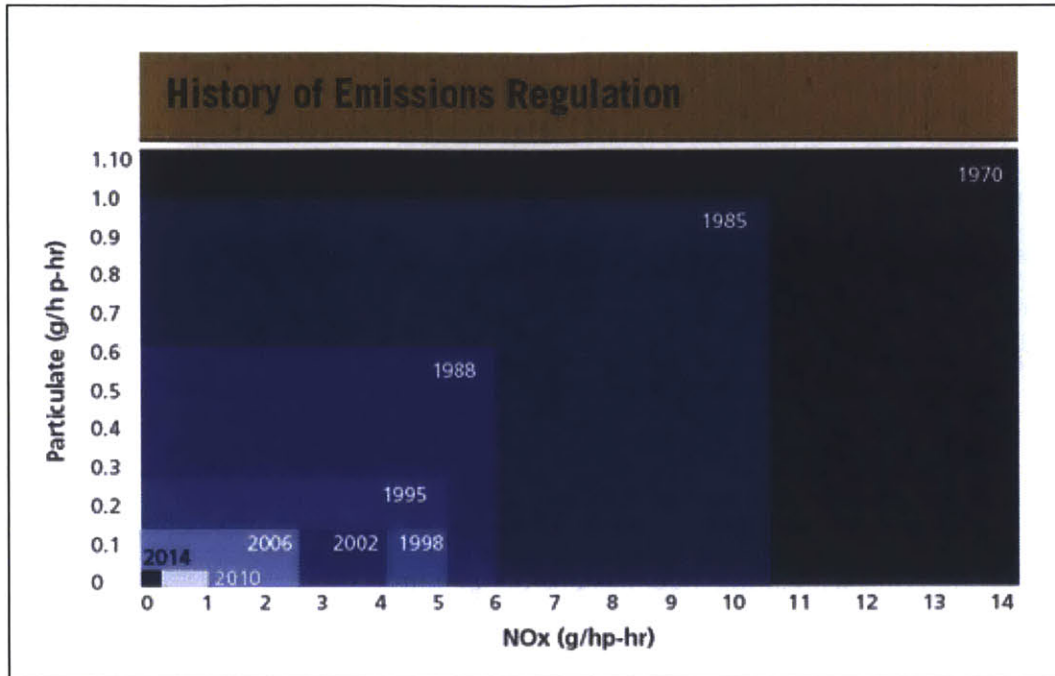


Figure 2: US Emissions Regulation (AGCO, 2013)

This tightening of emissions requirements is a double-edged sword but one with many positive effects. Nitric oxides are key contributors to pollution and are known to cause smog, acid rain, and organ damage. NOx also causes the formation of tropospheric ozone—a greenhouse gas that causes respiratory irritation, aggravation of asthma, and reduced lung function. Furthermore, particulate matter can be very bad for respiratory health (Pope 1995). This can be witnessed in developing countries with low levels of pollution regulation.

However, many times these positive effects come as a trade-off to engine performance. Components may be added with additional weight incurred or the engine may be tuned differently to meet regulations but reduce fuel economy and power. These quantities such as fuel economy and power directly affect the customer as well as his or her decision to purchase the vehicle. Furthermore, regulations may dictate which technologies come to the market. For example, direct injection (DI) is advantageous to combustion but is environmentally poor at cold start (Price 2007). Therefore, automotive manufactures are willing to invest in projects deliver utility to the customer while not sacrificing on emissions.



## 1.2 Control Strategy & Dilution

One technology that has shown promise to various degrees through the years has been dilution control. The principles of dilution are quite simple but implementation can be complex. For the purpose of this research, dilution refers to the addition of an inert substance to the combustion mixture. Dilution control was a technology developed in the 1970's as a means of reducing the nitric oxide emissions which is released at high combustion temperatures and to reduce pumping losses at part load.. Too much dilution, however, and the combustion stability of the engine is compromised. Misfire and excessive engine vibration lead to a very poor driver experience. It is known generically that NO<sub>x</sub> production scales exponentially with flame temperature, see Figure 3. This phenomenon is quite important in the use of dilution to control emissions.

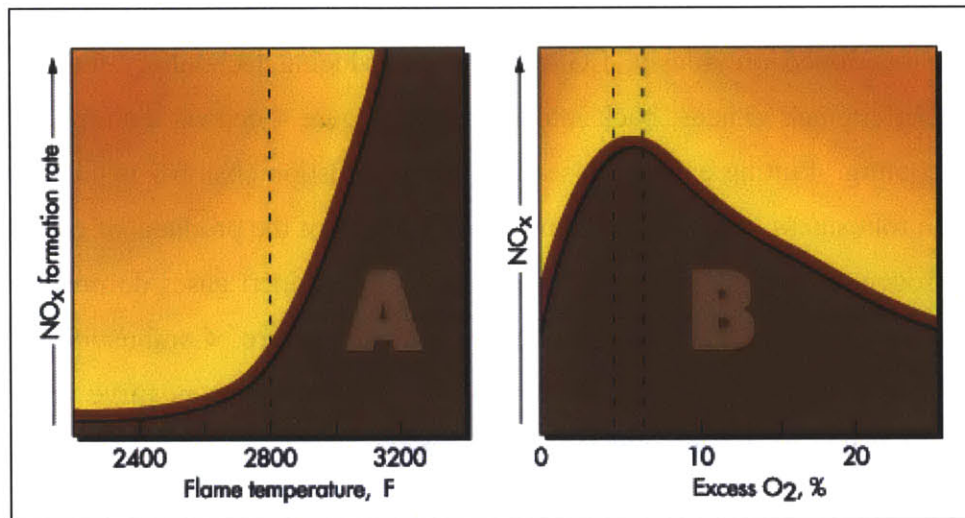


Figure 3: NO<sub>x</sub> formation rate (AlenTecinc.com)

Dilution was first brought about in the form of Exhaust Gas Recirculation (EGR) which redirects a portion of the exhaust back into the intake. In the early years of the technology, methods were crude and little control was achieved. It is now utilized in almost all cars in production. With advancement came new developments in dilution control. Many technologies currently being developed make use of other diluents such as water vapor (humidity) and air (lean combustion). The technologies and control strategies being explored include both hot and cold EGR, Homogeneous lean (Microstrat), stratified lean, and humidity compensation. Combustion is limited by the

composition and quantity of each diluent. The combustion robustness is commonly referred to as the combustion tolerance. This means that proper control strategies become very important. Too aggressive and the driver becomes inconvenienced by a poorly functioning engine. This research looks to the underlying combustion physics to see whether combustion outputs can be reasonably predicted. Engine related parameters such as load, speed, spark timing, valve timing, and EGR quantity can then be adjusted accordingly. Optimized quantities may include efficiency for maximum fuel economy; low CoV of torque for engine smoothness, and low NO<sub>x</sub> to abide with pollution regulation. CoV, or coefficient of variation, of torque will be explained further in a later section.

### 1.2.1 EGR

As mentioned previously, EGR is a NO<sub>x</sub> reducing technology that redirects a portion of an engine's exhaust back into its intake. Figure 4 depicts a simple EGR loop with intercooling. Putting exhaust gases into the combustion chamber is unfavorable for combustion robustness. EGR is a diluent which consists of the products of combustion—mainly nitrogen, carbon dioxide, and water vapor. These inert gases do not take part in the combustion reactions but lower the burned gas temperature. Combustion rate is thus reduced. However, there are also many positive effects. Both positive and negative aspects of EGR will be discussed in the following sections

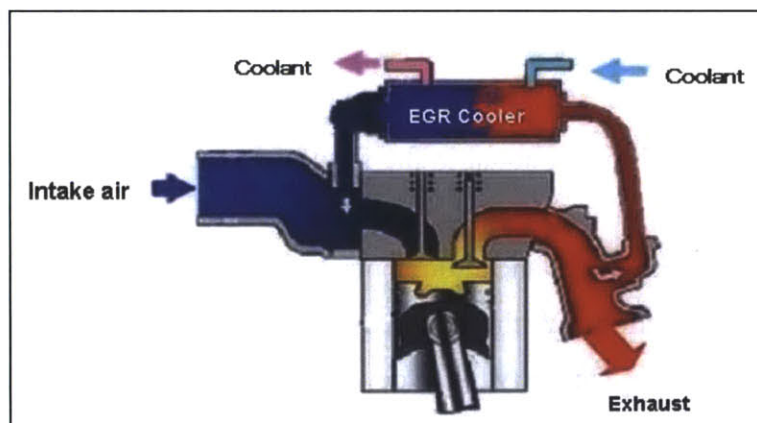


Figure 4: Schematic of EGR loop (Novinky, 2010)

Performance declines occur from a variety of effects. The first is that EGR reduces the combustible charge composition in the cylinder. This reduces peak power

because power is directly related to the quantity of air and fuel present in the combustion cylinder. Another effect is that EGR slows down combustion and increases the overall heat capacity which reduces peak combustion temperatures. Furthermore, as EGR is increased combustion quality diminishes and misfire becomes an issue. This point is often called the combustion tolerance. In general EGR is not used at idle (low load, low speed) or high load. This is because at idle, combustion becomes unstable. At high load, max power is desired and so EGR is not used.

Nonetheless, EGR is utilized because its positive effects outweigh the negative effects. There are number of pros that make EGR very favorable in today's auto market. First and foremost is the reduction in peak flame temperature. This occurs because of the additional heat capacity of the exhaust gases which are noncombustible. This reduction in peak combustion temperatures results in a significant decrease in NO<sub>x</sub> production. It was shown earlier in Figure 3 that NO<sub>x</sub> production scales exponentially with NO<sub>x</sub>. Running lean may seem to be a viable alternative but NO<sub>x</sub> production is increased by the availability of excess oxygen.

Besides the important reason of reducing emissions, EGR has secondary benefits. Reduced throttling losses are one of these. For an equivalent power output, the throttle must be open more to allow the passage of both the combustible charge and the exhaust gases. Manifold pressure is then higher resulting in a smaller pumping loop, see Figure 5. Another benefit is a reduction in heat losses. Heat losses are roughly proportional to the difference between the cylinder wall temperature and the engine coolant temperature. Thus lower combustion temperatures lead to lower wall temperatures and less heat losses. Furthermore, adding EGR changes the specific heat ratio which then changes the thermal efficiency. Higher specific heat ratios mean that more thermodynamic work can be extracted from the engine. The specific heat of EGR is less than that of air. Finally, there is a reduction in chemical dissociation at lower flame temperatures. Chemical dissociation is a breakdown of the chemical bonds at very high temperatures which decreases the useful energy released during the combustion process.

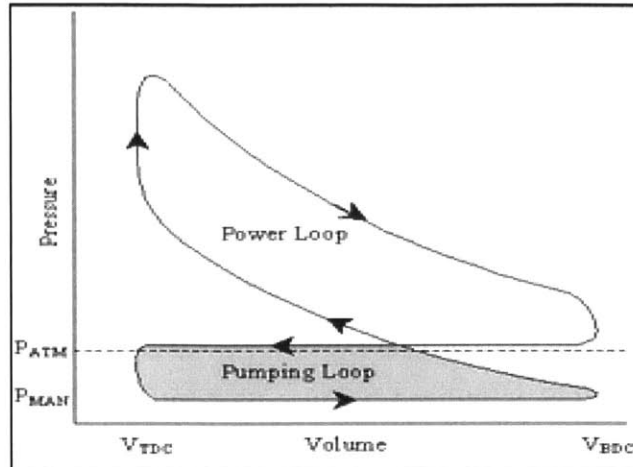


Figure 5: Pumping Loop (Mechadyne International 2012)

### 1.2.2 Lean Combustion

Lean combustion refers to the use of air-fuel ratios greater than stoichiometric (excess oxygen). The relative air-fuel ratio, lambda, is a very important quantity related to lean combustion. This is the ratio of the air-fuel ratio to stoichiometric. Phi, the inverse of lambda, is also commonly used. These terms have been defined in Equation 1. Research has shown that there are benefits to running an engine in the lean regime (F. G. Ayala 2006). For instance, increases in the net indicated specific fuel consumption are commonly observed. Similar to the use of EGR, much of the benefit is derived from the ability to reduce pumping losses. Engines are typically designed to reach a peak load and speed. Thus at non-peak conditions, lean combustion can allow the throttle to be open wider and result in reduced pumping losses. Another benefit is the higher specific heat ratio which improves fuel conversion efficiency.

$$\lambda = \left( \frac{A/F}{A/F_{Stoich}} \right) = 1/\phi$$

Equation 1

The biggest drawback of lean combustion is the emissions concern. Figure 6 shows the effect of the relative fuel-air ratio on combustion products. For instance, NOx production peaks slightly lean ( $\lambda \approx 1.1$ ) in the presence of some excess oxygen. This is seen in the right plot of Figure 3. Reduction in NOx is only achieved at very lean

conditions. Moreover, the modern 3-way catalytic converter does not perform well in the presence of excess oxygen. The catalytic converter relies on a series of oxidation and reduction reactions that require a given mix of exhaust gases to perform optimally. Therefore, stoichiometric operation has become the standard in modern automobiles.

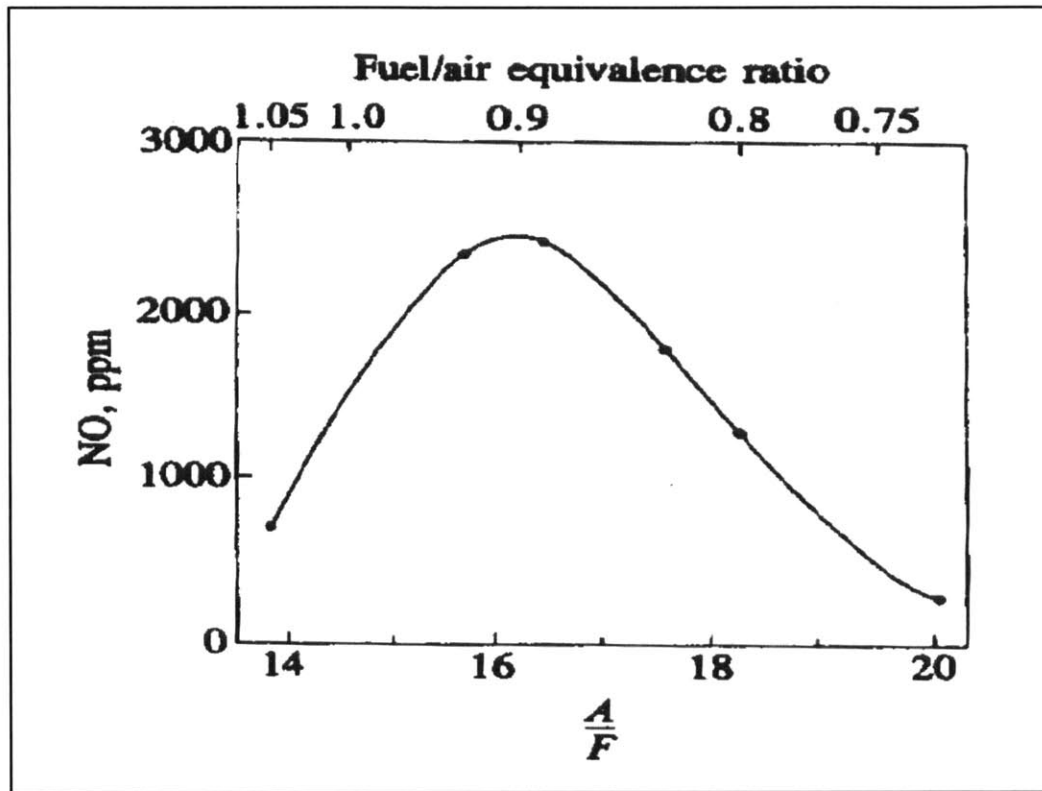


Figure 6: Variation of exhaust NO concentration with A/F and fuel/air equivalence ratio. Spark-ignition engine, 1600 rev/min,  $\eta_v = 50$  percent. (Heywood 1988)

### 1.2.3 Water Vapor Compensation

Water vapor compensation is another control strategy being explored by automotive companies. By adding more variables into the dilution control strategy, uncertainty is reduced and a more aggressive strategy can be justified. Humidity (water vapor) in the intake air has been ignored in the past. It plays a relatively small effect in the overall combustion process. Nonetheless, humidity is a diluent that contributes to the overall combustion tolerance. Water vapor content in the air can vary significantly depending on altitude, weather conditions, temperature, location, etc. Water vapor content in the air can be found by multiplying the relative humidity by the saturation

vapor fraction of water. Figure 7 provides a rough magnitude of these water vapor values while Figure 8 shows a rough map of the humidity zones in the United States. After a rain storm in Florida, there may be significant water vapor content in air while an arid region such as Arizona may have very little water vapor in the air.

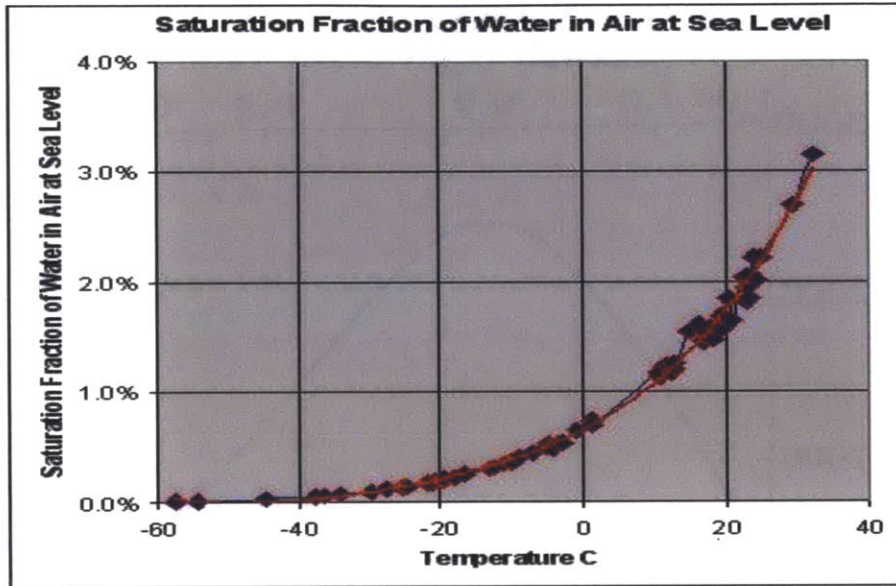


Figure 7: Atmospheric dewpoints versus temperature (Benson 2004)

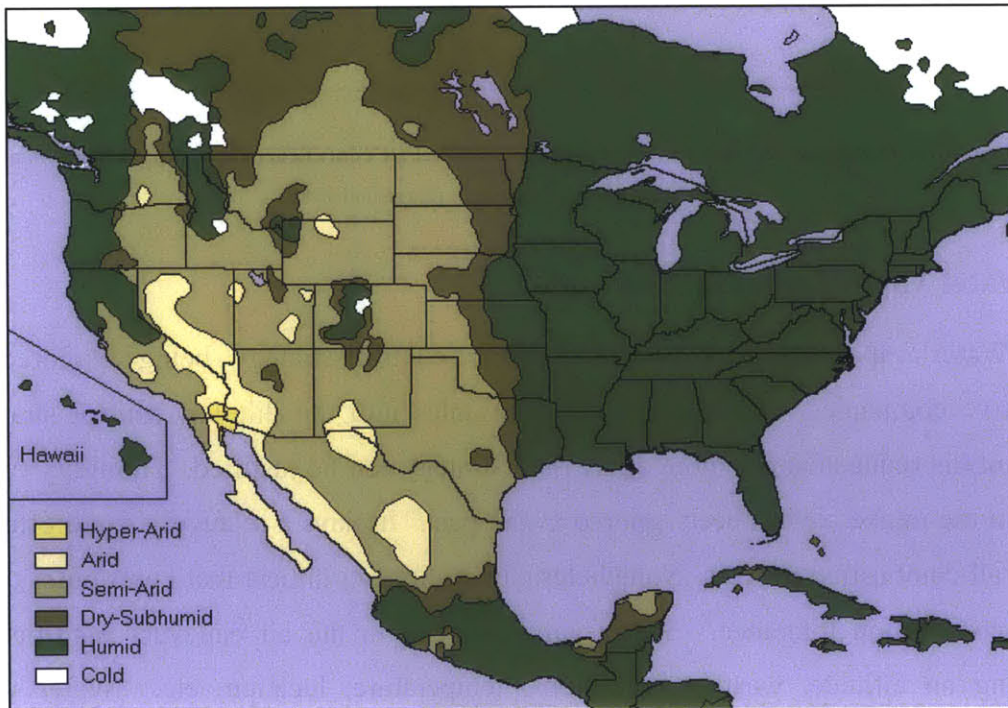


Figure 8: United States Humidity Zones (Tabor 2001)

### 1.3 Dilution Tolerance

As mentioned previously, there are a variety of diluents being explored. These include humidity control (water vapor), lean combustion (excess air) and EGR. For each diluent and combination of diluents there exists a dilution tolerance for the engine. The dilution tolerance is of course different for each individual diluent. The dilution tolerance is a measure of the engine's ability to cope with these noncombustible, inert fluids. Eventually there is the point that combustion does not occur and cycles begin to misfire. This point is often called the combustion limit.

Dilution tolerance is often measured using the coefficient of variation (CoV) of parameters such as the net indicated mean effective pressure or NIMEP. The coefficient of variation is a normalized parameter that measures the spread in the probability distribution.

NIMEP is a normalized parameter indicating the load of an engine. Its definition is given below. It is useful because it can be used as a comparison measure for different sized engines.

$$NIMEP = \frac{Work}{Displacement\ Volume} = \frac{W}{V_d}$$

Equation 2

Typical CoV of NIMEP for a smooth running engine is a few percent. At low dilution, this does not increase substantially. However, this value increases very rapidly near the combustion limit. This relationship has been studied extensively for both EGR (Alger 2007) and lean combustion (F. H. Ayala 2007), see Figure 9. This concavity which appears is a very important concept. In dilution control strategies it is essential to stay comfortably to the left of this sharp increase in CoV. High CoV is very undesirable and a nuisance from a driver's standpoint. Engine operation becomes rough with heavy vibration.

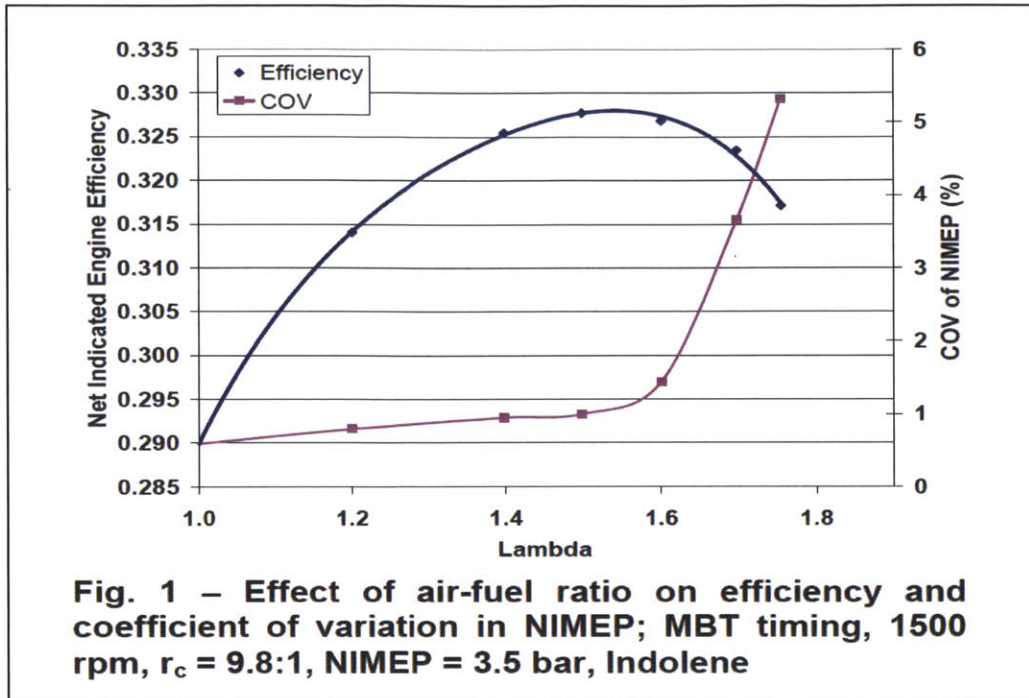


Figure 9: CoV and lambda

In theory, the combustion limit of an engine is a function of a key set of parameters including the specific heat capacity, pressure, and charge temperature. This makes it possible to determine the dilution tolerance of any diluents on a thermodynamic level. Previous research has linked combustion variability inversely with burn duration (F. H. Ayala 2007). Figure 10 shows the relationship between the 0-10% burn duration and CoV of NIMEP. Burn duration depends on the initiation of the combustion reactions and flame propagation. There are two major components to this: laminar flame speed and turbulent convection. Turbulent convection is largely a function of the engine and piston geometry. Laminar flame speed is a function of the trapped charge composition. It can reasonably be inferred then that there exists a relationship between the trapped charge composition and CoV / dilution tolerance.



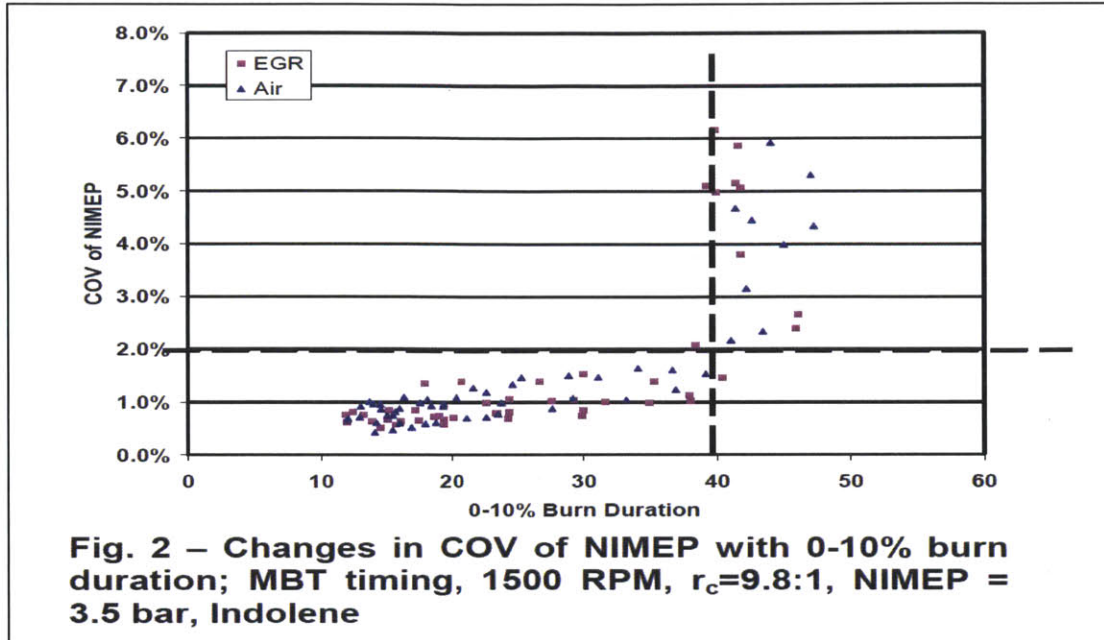


Figure 10: CoV for EGR and lambda sweeps

#### 1.4 Research Objectives

The purpose of this research was multifaceted. The overarching goal was to construct a practical model that translates the dilution tolerance of an engine for different diluents. The diluents to be analyzed were the three mentioned in previous sections—EGR, water vapor, and excess air. Previous research pointed to the conclusion that combustion outputs can be reasonably determined by understanding the combustion physics.

For this model to be useful in the real-world, certain inputs needed to be available. For the purpose of this study, the inputs were the diluent compositions, diluent quantities, and engine operating conditions. This chemistry can then be simplified into thermodynamic quantities such as charge temperature, pressure, and specific heat capacity. This simplifies things greatly because combustion chemistry is very complex. It requires systems of reactions, combustion kinetics, and equilibrium principles. There are, however, limits to the effectiveness of using only thermodynamics. The key outputs to this model were as follows:

1. CoV of NIMEP

2. Spark advance (under constant CA50)
3. Exhaust temperature
4. NO emission

This model was created using empirical data taken from experimentation. For the model to be of use to an automotive companies, it must be valid over a range of engine operating conditions. Testing was thus completed at three different speed and load combinations:

- (1) Low speed, low load (dilution is most sensitive)
- (2) Low speed, high load (typical driving condition)
- (3) High speed, high load (dilution may be unfavorable)

Experimental data was only taken for the three diluents and combination of the three, however, the model would work for any type of diluent.

#### **1.4.1 Choosing a lumped metric**

In order to facilitate the development of a model, it was decided to utilize a single metric that took into account the constituents of the trapped charge. This metric would then be used to correlate the experimental data for the key outputs. Thus in control strategies, this metric could be computed for any trapped charge composition to predict the outputs of combustion.

#### **1.5 Adiabatic Flame Temperature**

Adiabatic flame temperature was chosen as one possibility as a metric for the model. Adiabatic flame temperature is the temperature that results from complete combustion process without work, heat transfer or kinetic or potential energy changes. This process is depicted in Figure 11. The thermodynamics behind this quantity is quite simple. For adiabatic combustion under constant pressure, the enthalpy of the reactants (fuel and air) is equal to the enthalpy of the products (water vapor, carbon dioxide, and nitrogen). Adiabatic flame temperature neglects heat and work. In the adiabatic flame temperature calculation, 100% of the chemical enthalpy released in combustion is

absorbed by the change in sensible enthalpy between the products and reactants. The temperature at which this occurs is termed the adiabatic flame temperature.

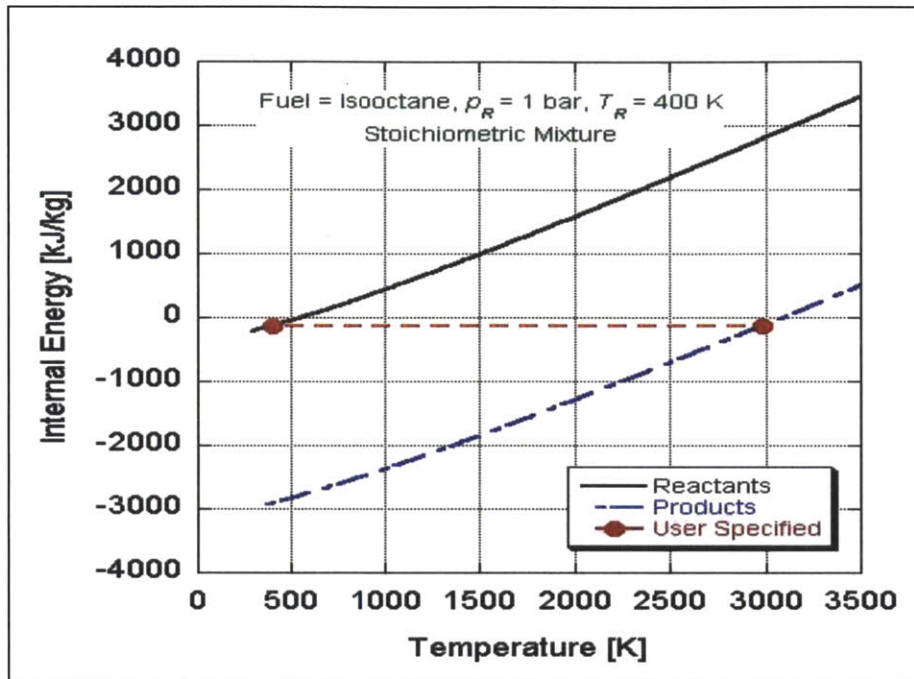


Figure 11: Adiabatic Flame Temperature, Isooctane (Depcik 2013)

In general, the adiabatic flame temperature reaches a maximum at stoichiometric, i.e. there is the exact amount of air to react with the fuel. Figure 11 shows a plot of this for isooctane. Any dilution such as excess air or exhaust gases decreases the flame temperature. This feature makes it a good metric for combustion tolerance. This also makes it a very valuable tool for this project. If the initial reactants are known then the adiabatic flame temperature can be attained. The initial reactants are known with only a small degree of uncertainty. EGR consists primarily of carbon dioxide, water vapor, and nitrogen gas; lean is excess air, and humidity control is added water vapor.

The one component that cannot be neglected however is the residual gases that remain in the combustion cylinder after each cycle. Residual gas fraction is largely a function of the engine speed/load. At normal running condition, residual gas composition is around 10%. At idle, this value might be as high as 25%. For the purposes of engine experimentation, this value is often hard to obtain. Engine modeling is one solution to this dilemma.

Adiabatic flame temperature was chosen for a variety of reasons. The first reason is that a fundamental metric was desired to model combustion. Adiabatic flame temperature is a single, independent metric that includes a vast amount of information pertaining to the trapped charge. In general, Equation 3 applies. Knowing temperature and pressure is difficult. A reference point was chosen to eliminate this difficulty.

$$T_{adiab} = f(T, P, C_p, \dots)$$

**Equation 3**

The second reason adiabatic flame temperature is a good metric is that it correlates linearly with laminar burning velocity. Figure 12 shows this relationship for propane combustion. Burning velocity has already been shown to be a good parameter to model combustion outputs such as CoV (Alger 2007). This correlation, however, breaks down when the reference condition  $(T_o, P_o)$  changes. In general, flame speed can be broken down into two parts: a temperature/pressure dependent component and a component evaluated at a reference condition, Equation 4.

$$S_L = S_{L,0} \cdot f(T, P)$$

**Equation 4**

Relating back to the phenomena illustrated in Figure 12, the reference flame speed can be defined as a function of adiabatic flame temperature evaluated at the reference conditions. See Equation 5.

$$S_{L,0} = f(T_{adiab}(T_u = T_o, P_u = P_o))$$

**Equation 5**

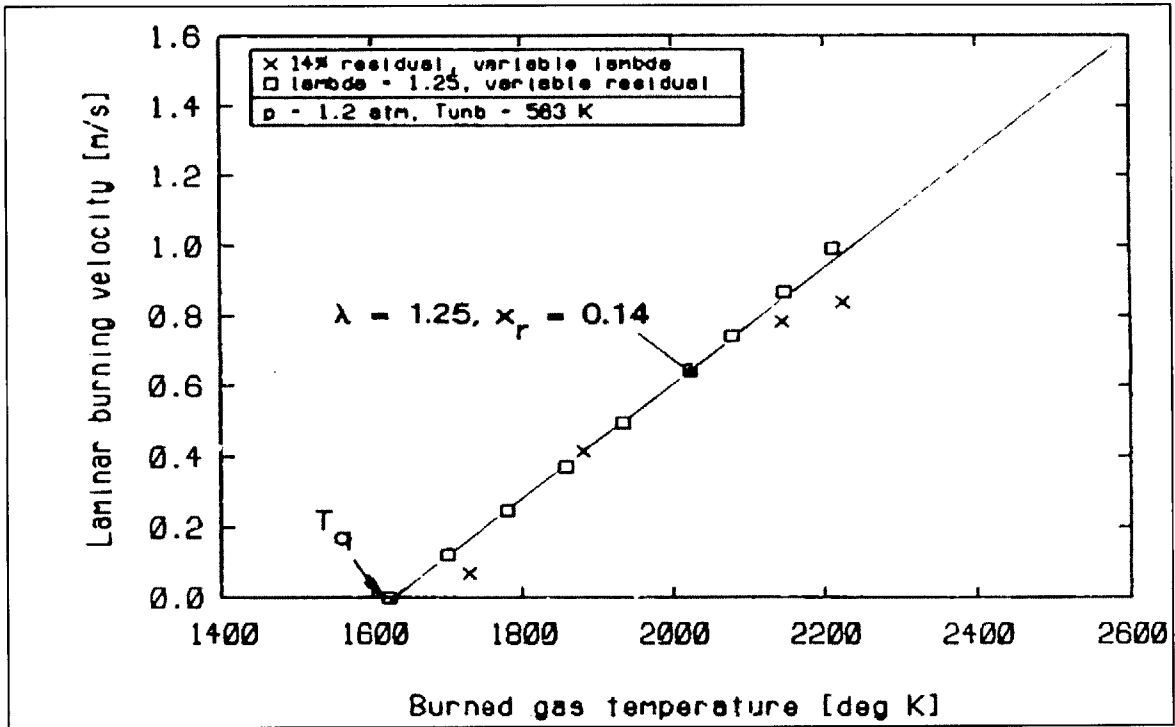


Figure 12: Burning velocity vs flame temperature; Propane,  $T_{unb} = 563$  K,  $P = 1.22$  bar (Pischinger 1985)

## CHAPTER 2 – EXPERIMENTAL METHODS

### 2.1 Test Engine Setup

For the experimental portion of this project, tests were conducted on a MY 2003 Chrysler 2.4 L four-cylinder SI engine. This is a dual overhead cam engine with port fuel injection (PFI). Engine specs are listed in Table 1.

<b>DaimlerChrysler 2.4 L – 4 Cylinders – Spark Ignition Engine</b>	
Cylinder Bore	8.75 cm
Crankshaft Stroke	10.15 cm
Connecting Rod Length	15.549 cm
Compression Ratio	9.542
Displaced Volume	610.34 cc
Intake Valve Open	1 degree BTDC
Intake Valve Close	231 degrees ATDC
Exhaust Valve Open	128 degrees ATDC
Exhaust Valve Close	8 degrees ATDC

Table 1: Test Engine Specs

To eliminate cylinder-to-cylinder interaction, this engine was modified to run only a single cylinder. Cylinder #4 was chosen to fire while Cylinders #1, 2, and 3 breathed air in and out but did not receive fuel or fire. Both the intake and the exhaust manifolds of the firing cylinder are separated from the non-firing ones.

#### 2.1.1 Dynamometer

The 4 cylinder Chrysler engine was coupled via a driveshaft to a dual-mode—motoring and absorbing dynamometer. This dynamometer utilized an eddy current with water braking. It was equipped with a Series 1000A dyno controller to control either

speed or load. It also had the ability to output speed to the data acquisition system as a voltage. Because testing was performed while only firing one cylinder, the dynamometer was mainly in absorption mode except in high load cases. Complete operating procedures for the engine and dyno setup are listed in APPENDIX A.

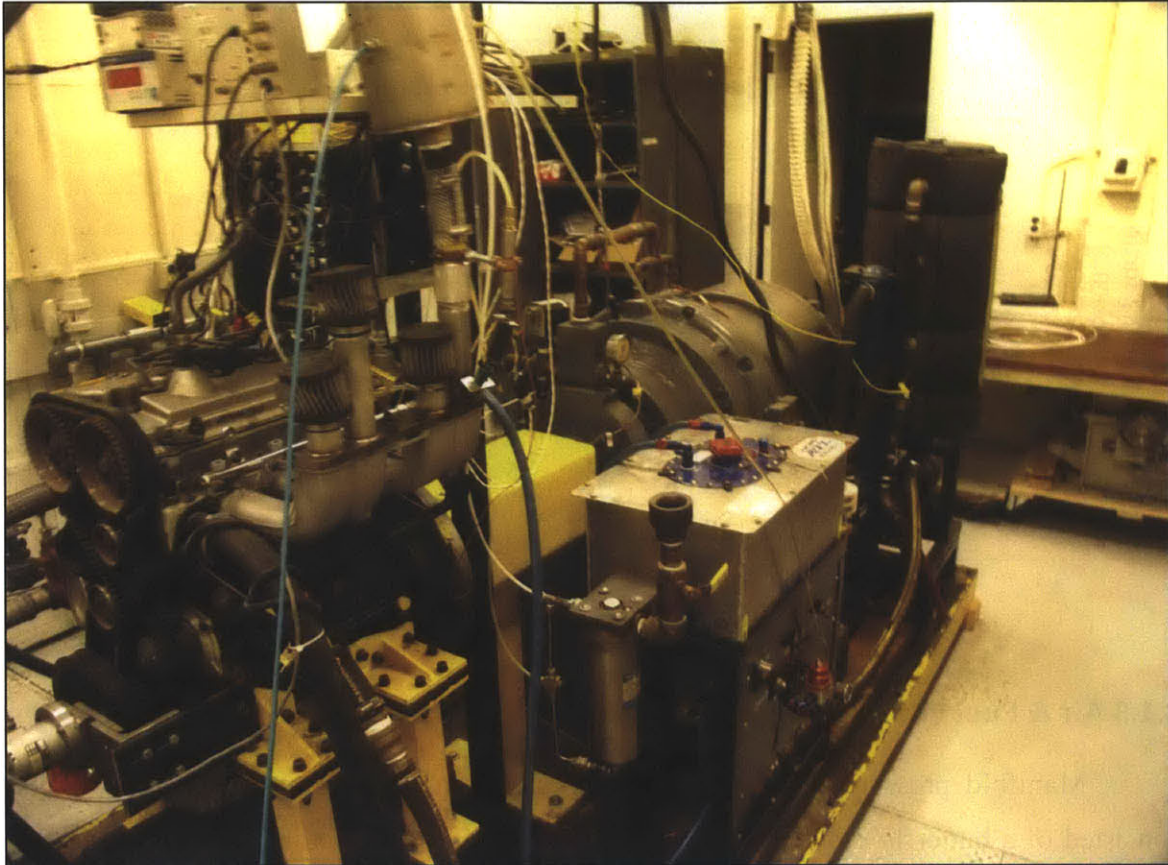


Figure 13: Engine/Dyno setup

### 2.1.2 Injection/Ignition Control

Because of the simplicity of only having one cylinder fire, injection and ignition were controlled using a custom setup. Typically an engine is equipped with an engine control unit (ECU) which makes use of a variety of sensors which provide feedback to control air, fuel, ignition timing, etc. In this setup, the control system was built using a custom C++ programmable interface. The inputs to the code were crank angle and bottom dead center (BDC) pulses which are provided by an encoder connected to the engine shaft. This provides timing reference which the code then uses to control injection and ignition. Injection is outputted via a pulse generator with which the duration of the

pulse corresponds to the amount of fuel injected. Spark timing is accounted for by setting both the charging duration of the ignition coil and the time at which ignition occurs. Thus by prescribing the ignition timing, injection timing, and fuel pulse width, the engine can be operated in a different load/speed conditions.

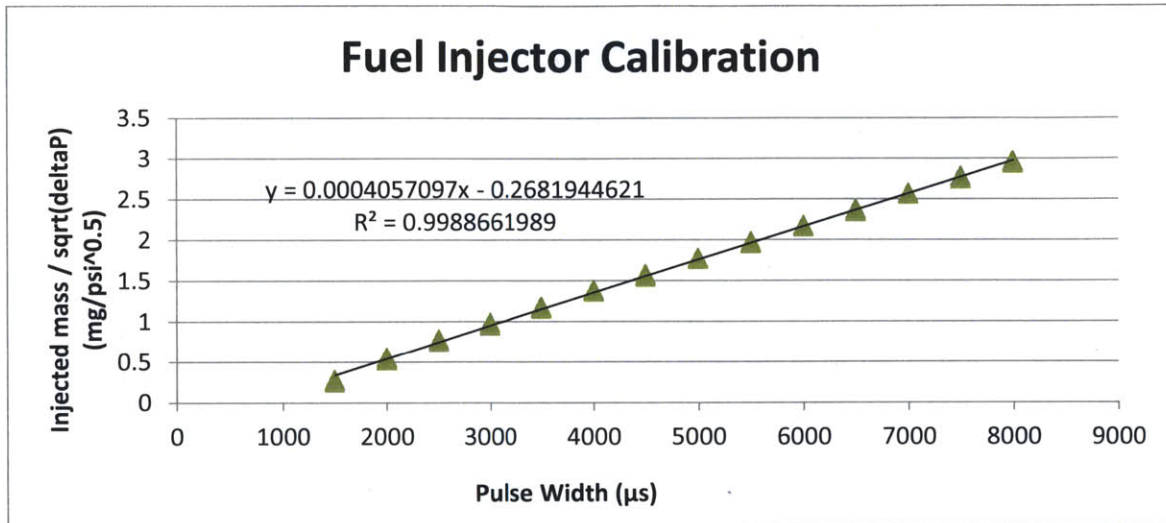


Figure 14: Fuel injector calibration for test engine

### 2.1.3 Air & Fuel Control / Measurement

Manifold pressure was adjusted using a custom built throttle controller. This consisted of a butterfly valve connected to a gear reducer and motor. This was used for open loop control of NIMEP. Exhaust gases were sampled using a Horiba MEXA-700λ Air/Fuel Analyzer. This is an emissions measurement system that is capable of measuring the air/fuel ratio, lambda, and oxygen percentage of lean, stoichiometric, and rich combustion regimes. In this case of the experimentation for this project, each individual test was conducted at a fixed air/fuel ratio. As a result, this measurement was incorporated in the Injection/Ignition Control C++ program discussed in 2.1.2 Injection/Ignition Control. Close loop control of lambda was achieved by adjusting fuel pulse width and injection timing.



#### **2.1.4 EGR Loop and CO<sub>2</sub> Measurement**

In a common automobile the exhaust gas recirculation circuit resembles that of Figure 4. The engine was retrofitted with an external EGR loop splitting the exhaust and redirecting it back to the intake. Control of the EGR rate was achieved by placing flow restricting valves in series with the EGR loop. This was done manually. Multiple valve were used for both course and fine adjustment. This enabled the correct amount of exhaust gas to be redirected into the intake. Furthermore, a thermocouple was placed at the just upstream of the junction where the exhaust gas and fresh gases mixed. Because the EGR loop was longer than a tradition setup, this temperature ensured that the water vapor in the exhaust gases did not condense. To measure the percentage of EGR in the intake an independent measurement was taken. Carbon dioxide was sampled from the intake using a Horiba MEXA-554JU. The measurement machine utilizes non-dispersive infrared and is capable of simultaneously measuring CO, HC, and CO<sub>2</sub>. The measurement setup used can be seen in Figure 15. The sample is pumped from the intake at sub atmospheric, condensed, dried, and finally throttled to atmospheric before being sampled by the Horiba measurement unit.

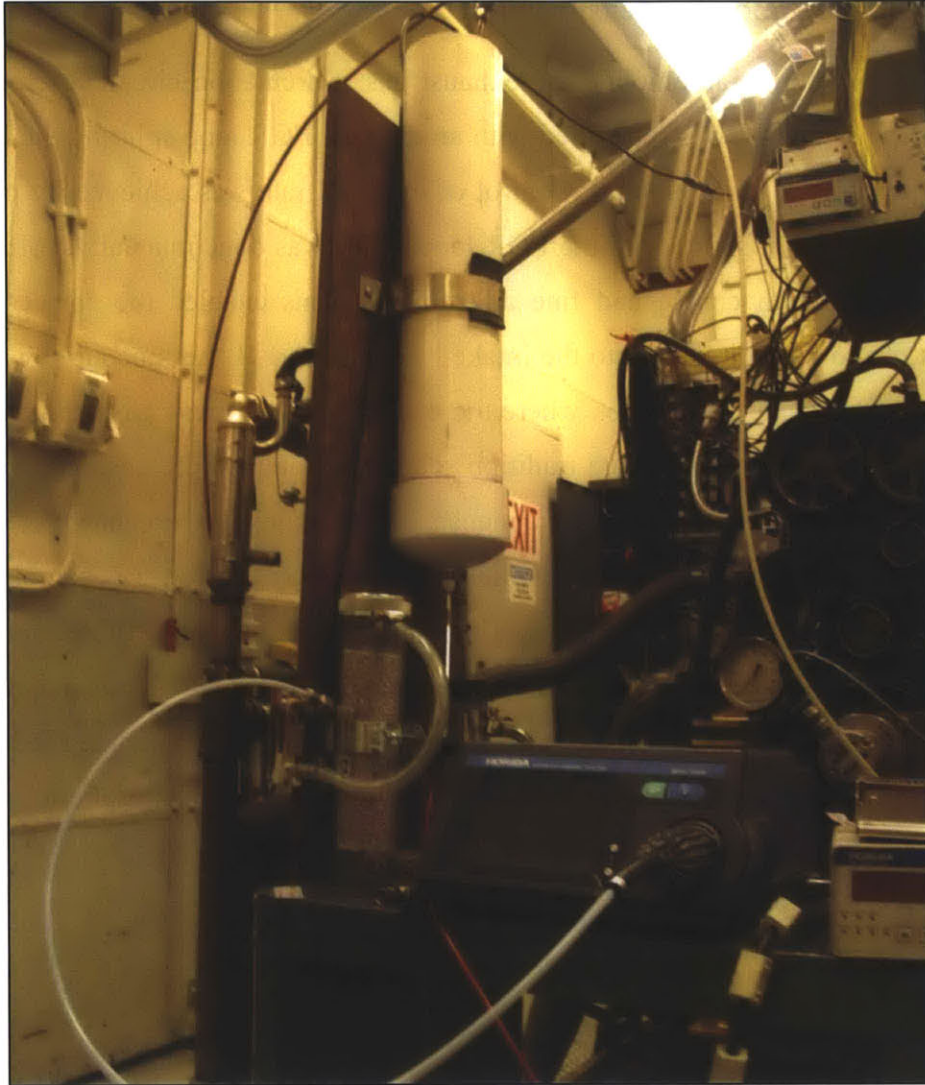


**Figure 15: CO<sub>2</sub> Measurement**

### **2.1.5 Water Vapor Injection**

A separate water storage tank was placed near the engine to supply water vapor dilution. This tank was pressurized with an external nitrogen tank at 60 psi and connected with Swagelok tubing to a fuel injector mounted in the intake manifold. This fuel injector (in this case being used as a water injector) was placed as close to the intake port as possible and at a low angle to the incoming flow to ensure proper mixing. This setup may not be optimal for dilution with water vapor but it provides good control over how much water was injected. Water injection could be controlled by both adjusting the pressure of the tank and adjusting the water pulse duration. Similar to the fuel injection

system discussed in 2.1.2 Injection/Ignition Control, the water injection was triggered by BDC pulses. Pulse width was controlled by an external waveform generator. No closed loop control schemes were used. Calibration was performed to ensure linear output with pulse width and square root output with changes in tank pressure, see Figure 16.

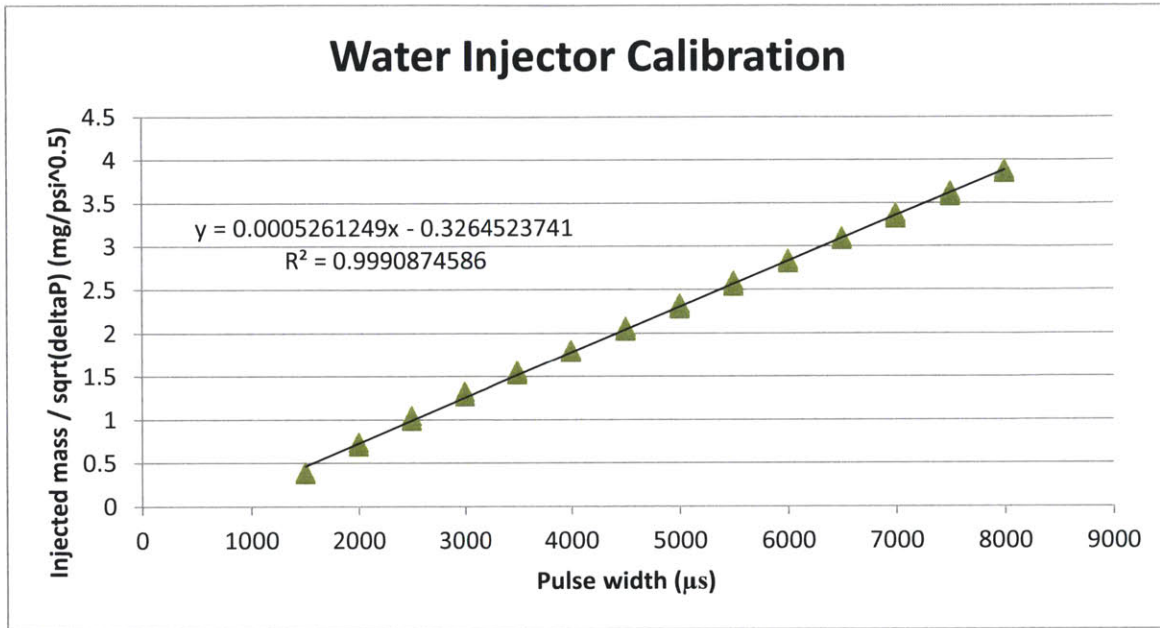


Figure 16: Water Injector Calibration

### 2.1.6 Cylinder Pressure Measurement

Cylinder #4 of the engine was equipped with a side mounted port to allow for a pressure transducer to be installed directly into the combustion chamber. The pressure transducer used for testing was a Kistler 6125A capable of measure pressures from 0 to 250 bar. The transducer is a piezoelectric device which when connected to a Kistler charge amplifier resulted in an output voltage. Calibration was performed using a deadweight testing device to translate the voltage to a pressure measurement. For the range of pressures used in testing (0-90 bar), this relationship is very linear, see Figure 17.

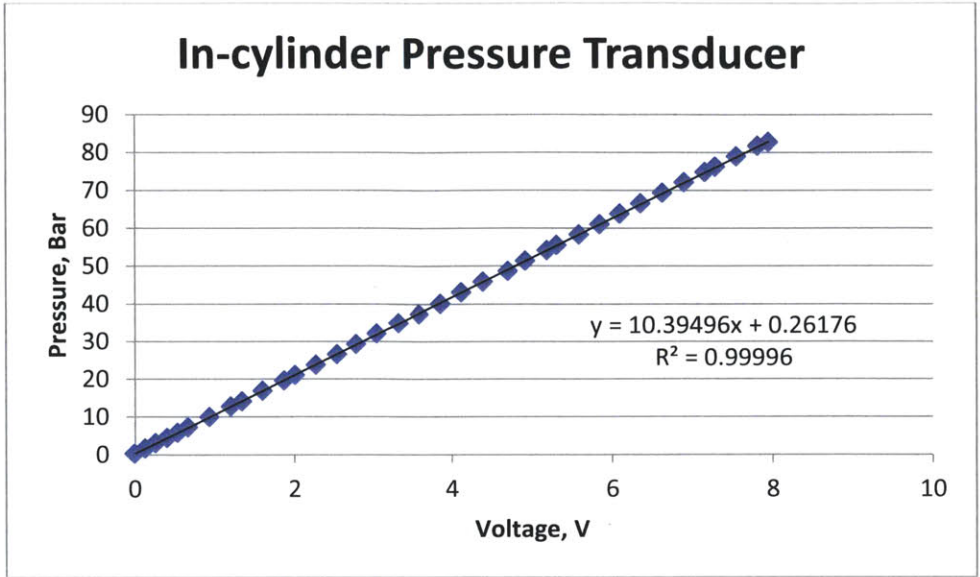


Figure 17: Pressure Transducer Calibration

### 2.1.7 Temperature Measurement

The test cell was equipped with an array of thermocouples for temperature measurements. Thermocouples were K type and manufactured by Omega. The K type thermocouple is constructed by a junction between chromel and alumel metals and ideal for temperatures ranging from -200°C to 1350° C. Temperatures measurements were performed at variety of places as listed in Table 2.

Channel Number	Thermocouple Location
0	Intake Temperature
1	Exhaust Temperature
2	EGR (at mixing point with intake air)
3	Engine Coolant
4	Ambient air

Table 2: Thermocouple locations

### 2.1.8 NOx Measurement

Exhaust gas was sampled in an exhaust damping tank for nitric oxide emissions using a Horiba MEXA-720NOx meter. This instrument operates via a zirconia ceramic sensor which is placed in direct contact with the exhaust gases. The sensor itself has a



Sampled 1/CA		Sampled 1/Cycle	
Channel Number	Sensor/Measurement	Channel Number	Sensor/Measurement
0	Crank Angle	5	NO Concentration (ppm)
1	Cylinder Pressure	6	Fuel Pulse Width
2	Manifold Absolute Pressure (MAP)	7	RPM
3	Lambda	8	Intake CO <sub>2</sub>
4	Exhaust Pressure	9	Intake CO

**Table 3: Measurement Channels**

## **2.3 Testing Methodology**

Testing methodology was simplified by dividing testing into two categories. The first was single parameter sweeps and the second was joint sweeps to analyze interaction effects.

### **2.3.1 Engine Experiments**

Below, in Table 4 through Table 7 are test matrices for this project. These test matrices will then be repeated for each of the 3 test cases outlined in 1.4 Research Objectives— those being speed/low load, low speed/medium load, and high speed/high load. The engine load is limited to 6 bar. Because the engine is not turbo-charged, there is not sufficient air to achieve a higher load when substantial dilution is used.

**Single parameter sweeps:**

EGR	0%	.....	30%
H <sub>2</sub> O	0%	.....	30%
$\lambda$	1	.....	1.4
Conditions: 3.6 Bar/1500 rpm, 6 Bar/1500 rpm, 6 Bar/3000 rpm			

**Table 4: Single diluent tests**

Where:

$$egr \equiv \frac{m_{egr}}{m_{air} + m_{egr}} \text{ and } h_{2o} \equiv \frac{m_{h2o}}{m_{air}}$$

**Dual parameter sweeps:**

	$\lambda = 1$	...	...	$\lambda = 1.4$
0% EGR	(Reference)			
:	3 Conditions: 3.6 Bar/1500 rpm, 6 Bar/1500 rpm, 6 Bar/3000 rpm			
:				
30% EGR				

**Table 5: Test Matrix, EGR + Lean**

	$\lambda = 1$	...	...	$\lambda = 1.4$
0% H <sub>2</sub> O	(Reference)			
:	3 Conditions: 3.6 Bar/1500 rpm, 6 Bar/1500 rpm, 6 Bar/3000 rpm			
:				
30% H <sub>2</sub> O				

**Table 6: Test Matrix, EGR + Lean**

	H <sub>2</sub> O = 0%	...	...	H <sub>2</sub> O = 30%
0% EGR	(Reference)			
:	3 Conditions: 3.6 Bar/1500 rpm, 6 Bar/1500 rpm, 6 Bar/3000 rpm			
:				
30% EGR				

**Table 7: Test Matrix, EGR + Water Vapor**

### **2.3.2 Combustion Phasing**

For the purposes of this project, all tests were conducted at constant CA50. CA50 is defined as the crank angle degree at which 50% of the fuel is burned. This CA50 value was fixed at 5 degrees retarded from MBT. MBT was computed at the reference condition using constant fuel and sweeping spark. Maximum power output was recorded at CA50 equal to approximately 7 degrees ATDC. By operating the engine retarded from MBT, higher dilution rates were able to be achieved as dilution significantly increases burn durations. To hold CA50 constant, spark timing was adjusted accordingly. This calculation was performed real-time in LabVIEW as well as post-processing in Matlab. Significant spark advance was required at high dilution levels.



## CHAPTER 3 – EXPERIMENTAL DATA ANALYSIS

During testing, data was recorded and saved to text files for a variety of measurements. Cylinder pressure, MAP, exhaust pressure, and lambda were recorded at each crank angle. Less time sensitive measurements such as NO concentration, dynamometer speed, CO<sub>2</sub> concentration, and temperatures were recorded once per cycle. Crank angle measurements were recorded for 100 cycles while once per cycle or 72,000 samples. Per cycle data was recorded for 1440 samples. The following sections summarize how the data files were processed.

### 3.1 NIMEP

In the data processing routine, in-cylinder pressure data was pegged at BDC compression using the average MAP near BDC. This was performed on a cycle by cycle basis and averaged over the 100 samples that were taken. A sample pressure trace is shown in Figure 19. NIMEP was calculated from pressure data as shown below:

$$NIMEP = \int p \cdot dV = \int p \cdot \frac{dV}{d\theta} \cdot d\theta$$

Equation 6

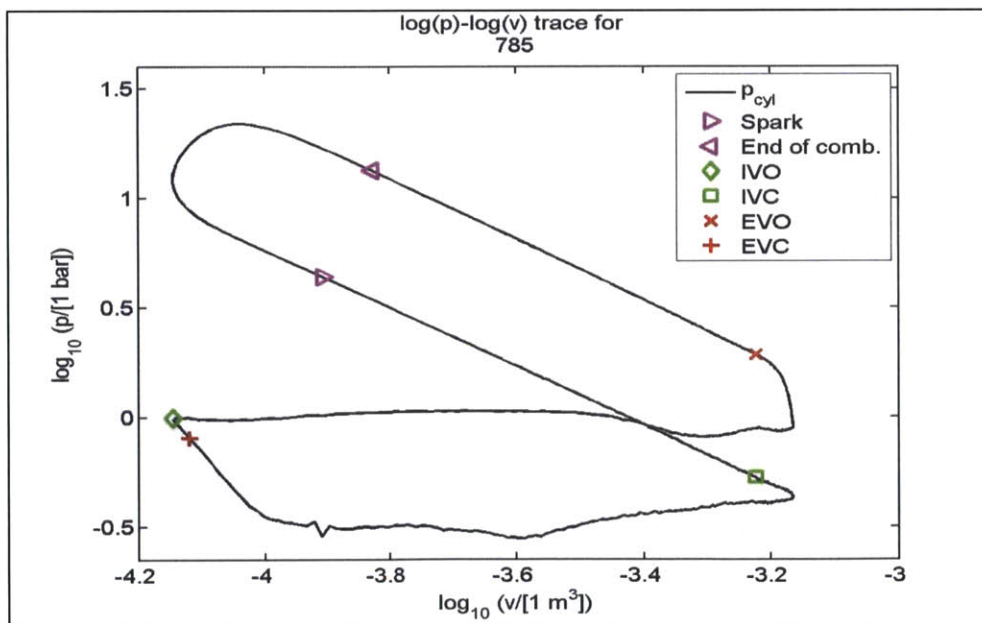


Figure 19: Pressure trace at part load

### 3.2 CoV of NIMEP

CoV can be calculated for any measured quantity. For this study, CoV of NIMEP was important because it measures variation between cycles of combustion performance. The standard equation is given below in Equation 7.

$$CoV = \frac{\text{standard deviation}}{\text{mean}} = \frac{\sigma}{\mu}$$

Equation 7

Furthermore, it was valuable to look at the histogram of NIMEP for high dilution cases with misfire. Figure 20 shows a histogram of NIMEP for a high dilution, high load EGR case. The histogram bar between NIMEP of -1 to 0 indicates misfire. Initially it was decided to remove the cycles with NIMEP less than half the mean value and calculate CoV for the other remaining cycles. Later, it was found that when this is done, it not only computes a much lower CoV, but it removes valuable engine information. High dilution leads to misfire and high CoV so ignoring misfire neglects the effects of dilution. In the end, it was decided that when doing the correlations, tests with CoV greater than 15% would be removed.

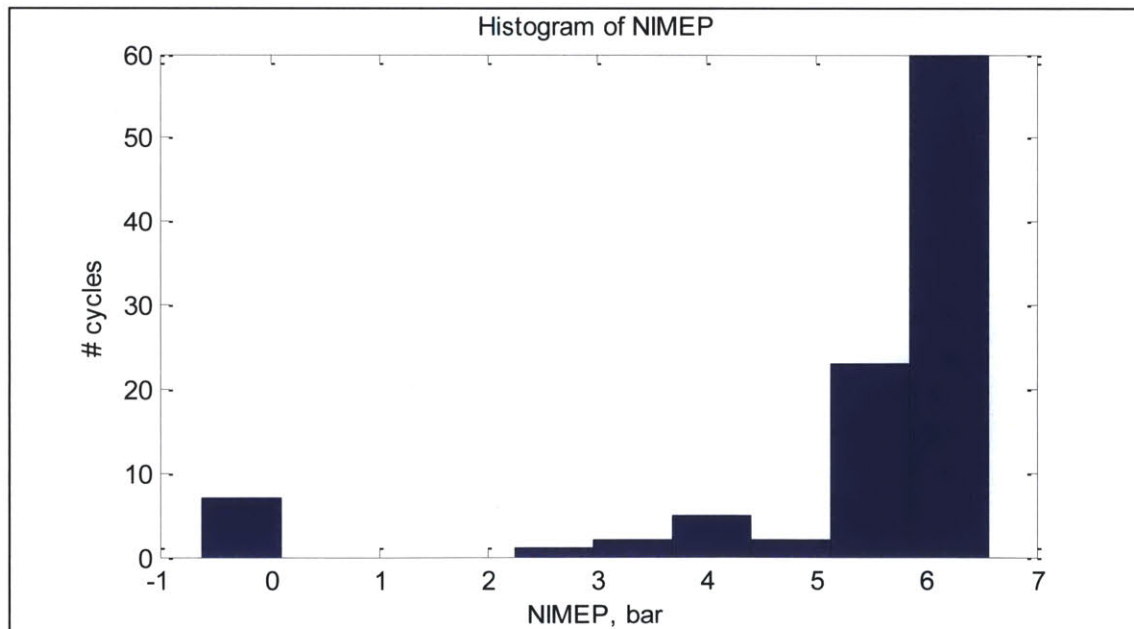


Figure 20: Sample Histogram of NIMEP

### 3.3 Heat Release Profiles

Heat release analysis was performed using the Rassweiler Withrow method first developed in 1938. It was used both in real-time to hold CA50 constant and in post-processing to verify its accuracy. The method was advantageous because of its ease of implementation and computational efficiency. The method works by dividing the pressure rise into two parts: pressure rise due to compression and pressure rise due to combustion (Mendera 2002). It then uses polytropic relations to compute the mass fraction burned. Error can result from the need to fix the beginning and end of combustion. However, this is quite small because combustion rates are the start and end are low. Sample traces are provided in Figure 22 for the MFB and apparent heat release for a test ran at part load.

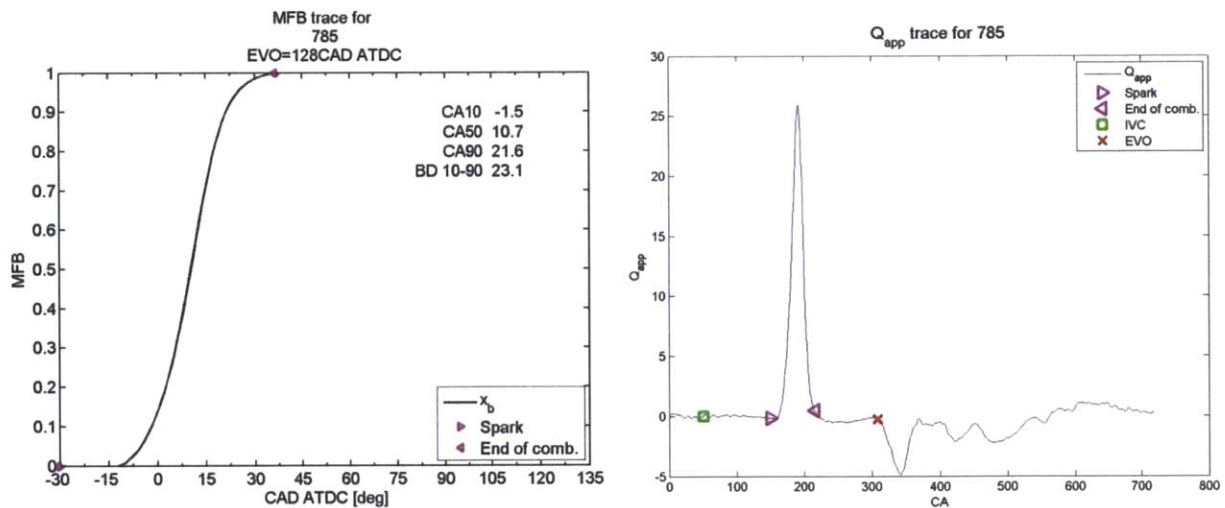


Figure 21: MFB and Qapp trace for test at part load

### 3.4 Specific NOx

In order to normalize NOx production which is measured by the sensor in mole fraction of parts per million, it was converted to a grams per unit work basis. A function was written in Matlab to compute this value. The equation below shows this calculation.

$$NOx \left[ \frac{\text{grams}}{\text{kW} - \text{hr}} \right] = \frac{\text{mass NOx}}{\text{work}} = \frac{x_{NOx} * \text{mass}_{total} * MW_{NOx} / MW_{exh}}{NIMEP * V_d}$$

Where  $x_{NO_x}$  is the mole fraction of NO<sub>x</sub>.

### 3.5 EGR Determination

The EGR value is defined by:

$$EGR = \frac{m_{EGR}}{m_{EGR} + m_{air}}$$

Equation 8

EGR was calculated from the intake and exhaust CO<sub>2</sub> measurements using a NDIR sensor after water is removed from the gas stream. The measurements are corrected for the known exhaust and ambient water vapor concentrations. To obtain wet values, the ambient CO<sub>2</sub> concentration is also subtracted. Then, if  $x = \text{intake CO}_2 \text{ mole fraction}$  and  $x' = \text{exhaust CO}_2 \text{ mole fraction}$ , the molar dilution ratio is as follows:

$$(EGR)_{molar} = \frac{N_{EGR}}{N_{EGR} + N_{air}}$$

Where N denotes the number of moles. The mass dilution ratio is then:

$$EGR = \frac{m_{EGR}}{m_{EGR} + m_{air}} = \frac{\frac{W_b}{W_a} \left( \frac{x}{x' - x} \right)}{1 + \frac{W_b}{W_a} \left( \frac{x}{x' - x} \right)}$$

Where  $W_b$  and  $W_a$  are the molecular weights of the burned gas and air respectively.

The plot in Figure 22 depicts this relationship between dry intake CO<sub>2</sub> and EGR for an EGR sweep at the stoichiometric air/fuel ratio.

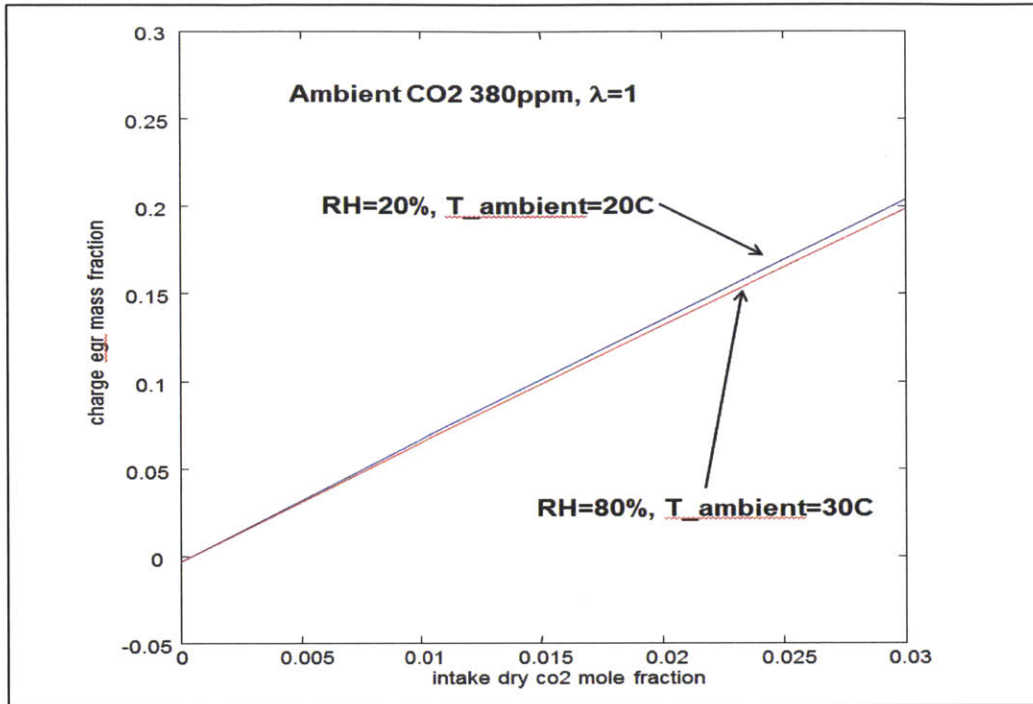


Figure 22: EGR vs CO<sub>2</sub>

### 3.6 NISFC

NISFC or net indicated fuel consumption is common measure of fuel efficiency. It is defined in Equation 9.

$$NISFC = \frac{\text{fuel consumption rate}}{\text{power}} = \frac{m_{\text{fuel}}}{NIMEP * VD}$$

Equation 9

## CHAPTER 4 – GTP MODELING

### 4.1 GT-Power Overview

A significant portion of this project involved gaining an understanding of the thermodynamics behind dilution control. For this, the engine simulation modeler, GT-Power, proved to be a very valuable tool. GT-Power is part of the larger set of engine and component simulation tools, GT-Suite, developed by Gamma Technologies. It has a wide range of applications. For this project, it was used as a simulation tool for modeling the breathing and combustion of an engine. The software uses iterative methods to achieve convergence in mass, temperature, and pressure along with user defined parameters. More specifically, it was used to compute the internal residual gas fraction. This is because there was no measurement system in place on the physical engine setup for measuring internal residual gas.

For the purposes of computing the residual gas fraction, an accurate engine model needed to be produced. To accomplish this, the 4 cylinder SI engine with EGR controller example in GT-Power was modified (Figure 23). The major changes were as follows.

- (1) CAM timing and valve lift profiles. The original engine used for testing had a small amount of valve overlap (angle between exhaust valve closing and intake valve opening). This needs to be modeled accurately because the internal residual gas fraction is highly depended on valve overlap. Valve overlap greatly increases the internal residual gas fraction.
- (2) Combustion phasing. Dilution plays a large factor in combustion phasing. Tests for this project were conducted at 5 degrees retarded from MBT. For the GT-Power model, the MBT point was first found and then 5 degrees was added. A wiebe curve was used to model the combustion and CA50 was fixed at this value. The burn duration, defined in the model as 10%-90% was extracted from the real engine testing data. These values were computed from engine cylinder pressured data via the Rassweiler Withrow method.
- (3) Water injection. Similar to the physical engine used during testing, fuel injectors were added to the intake port of each cylinder for the purpose of water

injection. The amount of water injected was metered as a fraction of the intake air flow.

- (4) EGR control. External exhaust gases were redirected back into the intake and controlled by a valve. PID control was used on this valve to achieve the correct fraction of external EGR in the trapped charge. Control needed to be set very conservatively because instabilities were common at higher levels of dilution.

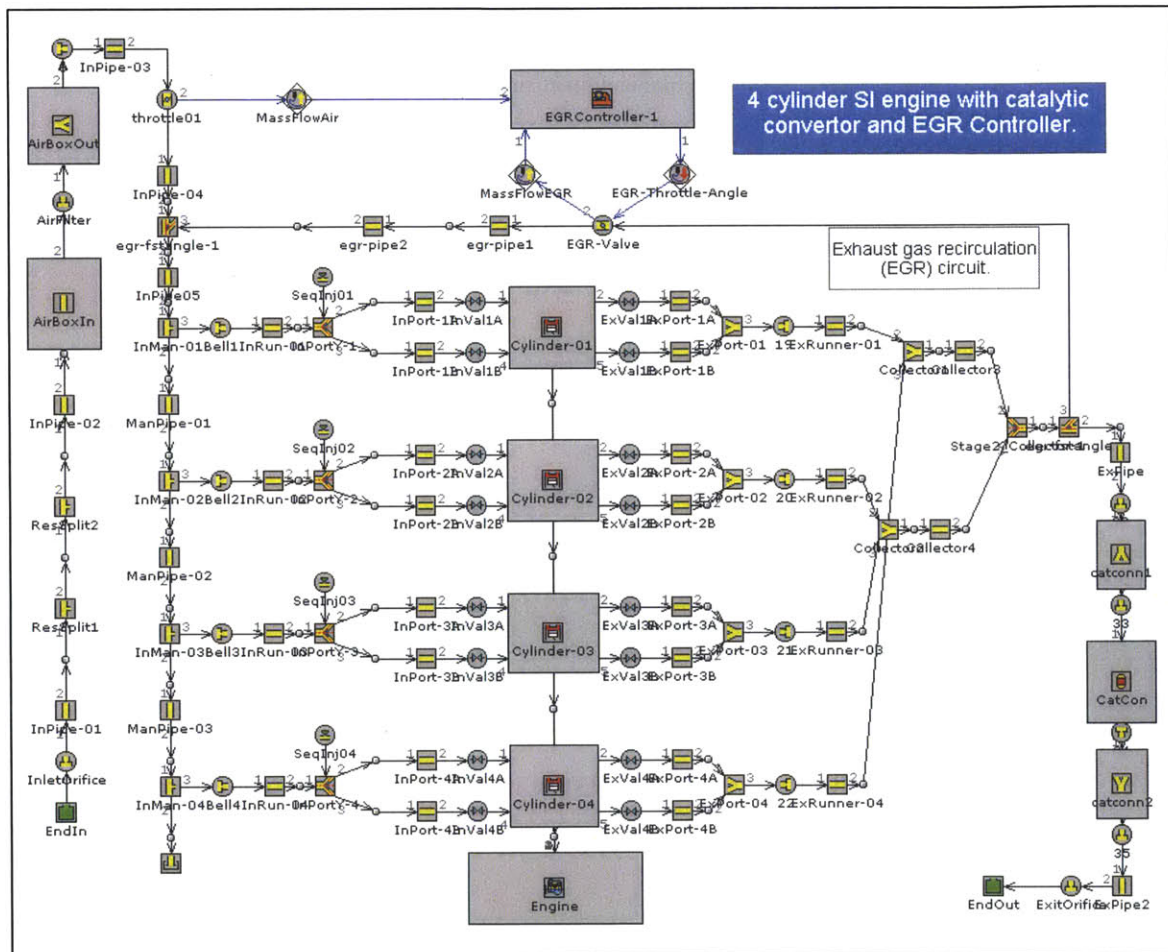


Figure 23: GT-Power Model

## 4.2 Model Matrices:

### Single parameter sweeps:

EGR	0%	5%	10%	15%	20%	25%	30%		
H <sub>2</sub> O	0%	5%	10%	15%	20%	25%	30%		
$\lambda$	1	1.05	1.1	1.15	1.2	1.25	1.3	1.35	1.4
Conditions: 3.6 Bar/1500 rpm, 6 Bar/1500 rpm, 6 Bar/3000 rpm									

Table 8: Single diluent simulation

### Dual parameter sweeps:

	H <sub>2</sub> O = 0%	H <sub>2</sub> O = 5%	H <sub>2</sub> O = 10%	H <sub>2</sub> O = 15%	H <sub>2</sub> O = 20%
0% EGR	(Reference)  3 Conditions: 3.6 Bar/1500 rpm, 6 Bar/1500 rpm, 6 Bar/3000 rpm				
5% EGR					
10% EGR					
15% EGR					
20% EGR					

Table 9: EGR+ H<sub>2</sub>O simulation

	$\lambda = 1$	$\lambda = 1.1$	$\lambda = 1.2$	$\lambda = 1.3$	$\lambda = 1.4$
0% EGR	(Reference)  3 Conditions: 3.6 Bar/1500 rpm, 6 Bar/1500 rpm, 6 Bar/3000 rpm				
5% EGR					
10% EGR					
15% EGR					
20% EGR					

Table 10: EGR+  $\lambda$  simulation

	$\lambda = 1$	$\lambda = 1.1$	$\lambda = 1.2$	$\lambda = 1.3$	$\lambda = 1.4$
0% EGR	(Reference)  Conditions: 3.6 Bar/1500 rpm, 6 Bar/1500 rpm, 6 Bar/3000 rpm				
5% EGR					
10% EGR					
15% EGR					
20% EGR					

Table 11:  $\lambda$  + H<sub>2</sub>O simulation



### 4.3 Model Results

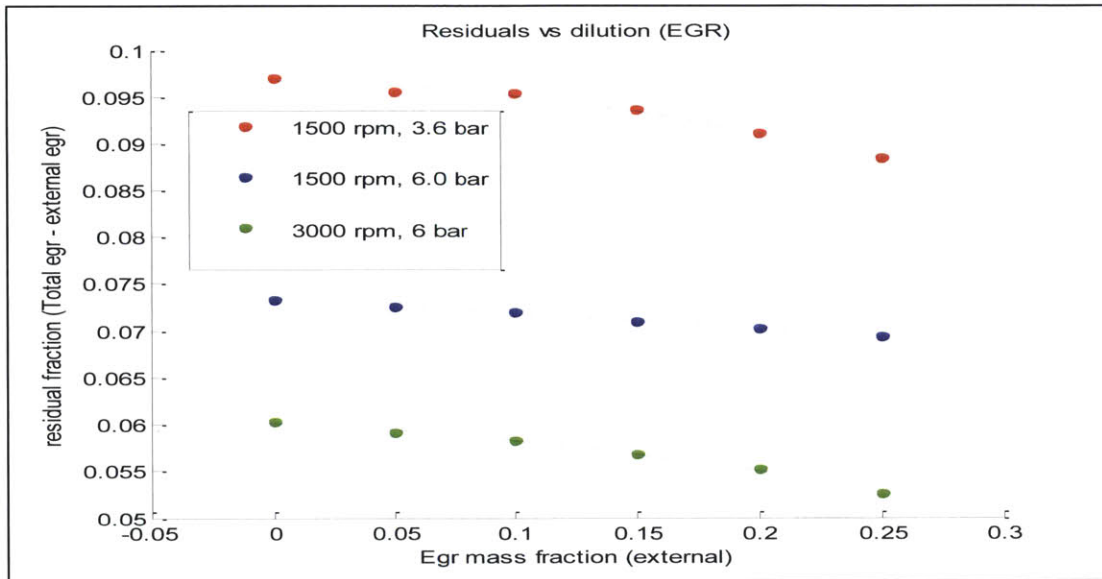


Figure 24: Residual gas composition – EGR sweep

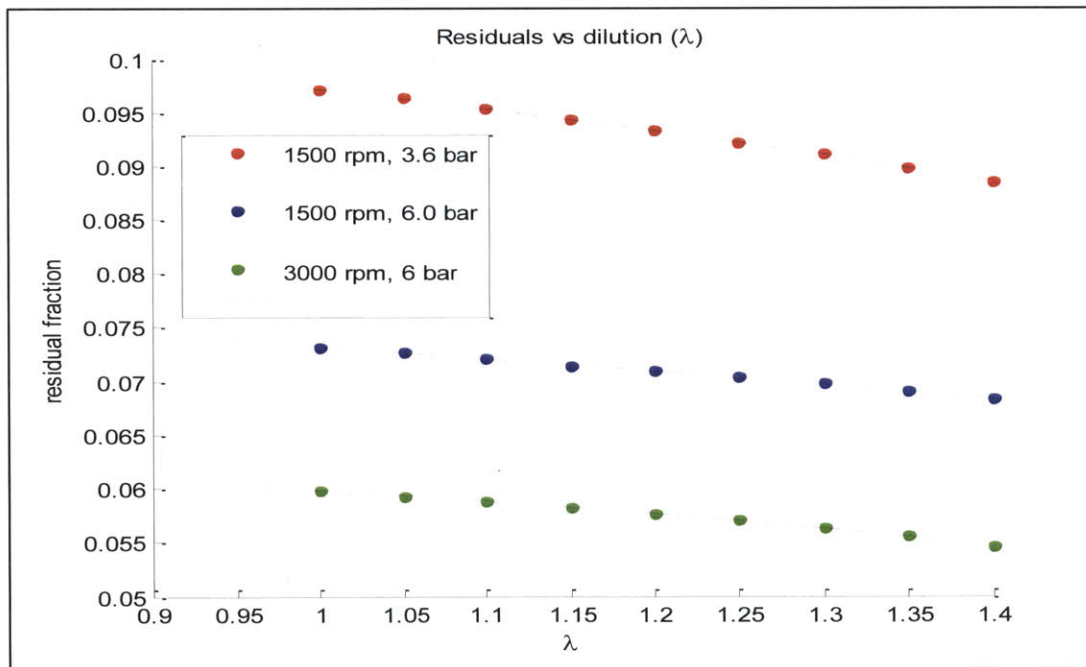
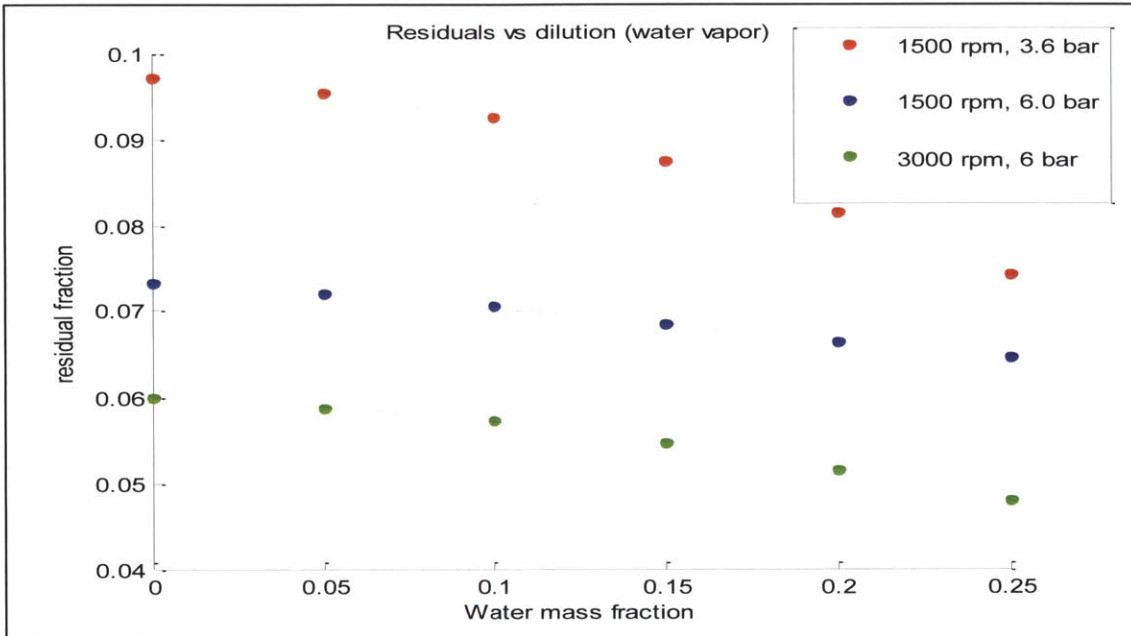


Figure 25: Residual gas composition – lambda sweep



**Figure 26: Residual gas composition – water vapor sweep**

These results in Figure 24 through Figure 26 show that residual gas fraction decreases with dilution such as water vapor, EGR, and excess air. One important reason for this is higher intake pressures occur because this is for constant NIMEP. Fuel is approximately the same for each case but dilution adds non-combustible gas to the mixture. Thus the engine is less throttled and the back flow of exhaust gas to the intake during the valve overlap period is reduced. Hence the residual gas fraction decreases with dilution.

The results also show that residual gas fraction differs depending on the operating condition. Following similar logic as before, residual gas fraction decreases with speed and load. In the case of this simulation, this change is dominant over the dilution effect. At zero dilution, the high speed, high dilution case has around 6% residual gas while the low speed, low load case has almost 10% residual gas fraction.

## CHAPTER 5 – Results

Multiple methods were used to correlation an independent variable to the targeted output quantities. These target output quantities are the following:

5. CoV of NIMEP (data points with CoV > 15 removed)
6. Spark advance (under constant CA50)
7. Exhaust temperature
8. NO emission
9. NISFC.

Correlation was attempted using a variety of metrics:

1. Adiabatic flame temperature.
2. Ford's EGR-Intake-Equivalent.
3. Linear combination of diluents

### 5.1 Adiabatic Flame Temperature

Adiabatic flame temperature was the first metric chosen for correlation. Intuitively this metric makes a great deal of sense. It effectively captures the combustion properties of the trapped charge and correlates linearly with flame speed. To calculate adiabatic flame temperatures, the trapped charge composition first needs to be determined. Then a reference condition (temperature and pressure) was selected and finally a method of computing enthalpies was needed. These calculated is outline in the following sections.

#### 5.1.1 Trapped Charge Composition

Adiabatic flame temperature was calculated for each testing point from the trapped charge composition. For each composition element, the mole fraction was computed based upon the intake and residual concentrations. The mole fraction for species  $i$  in the charge is given by Equation 10.

$$x_i = \text{Residual Fraction} * x_{i-\text{exhaust}} + (1 - \text{Residual Fraction}) * x_{i-\text{intake}}$$

#### Equation 10: Trapped charge mole fraction computation

Only a limited number of species were included in this trapped charge composition. These include  $N_2$ ,  $O_2$ , fuel, CO,  $H_2$ , and  $H_2O$ . The residual gas fraction and external EGR consisted primarily of  $CO_2$  and  $H_2O$ , trace amounts of  $H_2$  and CO, and excess  $N_2$  and  $O_2$  in the lean cases.

#### 5.1.2 Reference Condition

For the purpose of this research, the reference point for adiabatic flame temperature was selected to be pressure of 1 bar and temperature of 300 K. The reference point has the potential to affect the magnitude of flame temperature. Flame temperature is the temperature at which the enthalpy of the products equal the enthalpy of the reactants evaluated at the reference pressure/temperature. Thus increasing the reference temperature increases the flame temperature. Figure 27 shows the effect when different references points are used to calculate the adiabatic flame temperature. It is seen that while the magnitude of the temperature changes, the overall trend remains largely the same. For this correlation metric to be useful, a single reference point is most valuable. This simplifies its use in control strategy. In the case of using spark as a reference point, the temperature and pressure needed to be calculated using polytropic relations from the pressure trace. This would be highly impractical in an engine control strategy as it requires significantly more complex computation.

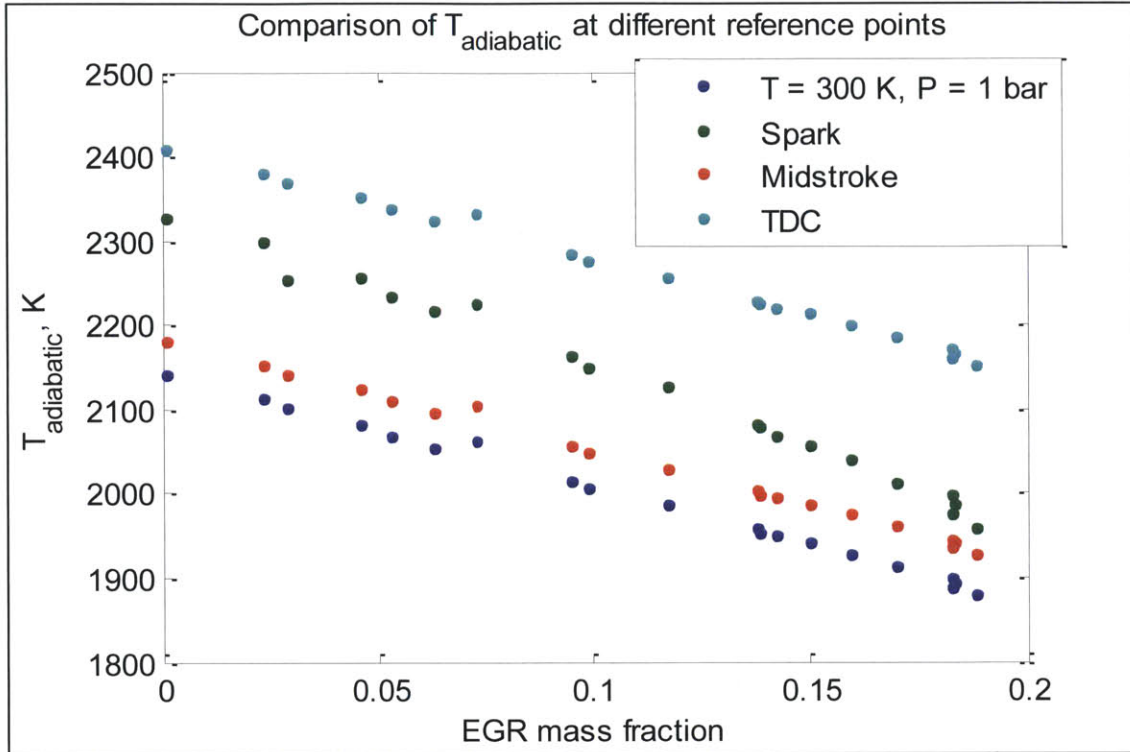


Figure 27: Adiabatic Flame Temperature comparison at 1500 rpm, 3.6 bar NIMEP

### 5.1.3 Calculation Method

Adiabatic flame temperature was calculated using an approach taken from a NASA equilibrium program (S. M. Gordon 1994). The approach is used to represent JANAF table thermodynamic data. It assumes both that the unburned mixture is frozen in composition and the burned mixture is in equilibrium (Heywood 1988). Thermodynamic properties which are a function of temperature are fitted with a polynomial curve. For example, enthalpy can be expressed as follows:

$$\frac{H_i^o}{RT} = a_1 + \frac{a_2}{2}T + \frac{a_3}{3}T^2 + \frac{a_4}{4}T^3 + \frac{a_5}{5}T^4 + \frac{a_6}{T}$$

Equation 11 (S. M. Gordon 1976)

These coefficients  $a_1 - a_6$  are known for a variety of species, see Figure 28. The burned gas species are assumed to be in equilibrium. Thus by fixing the reference condition, the final temperature of the species can be solved for. This final temperature was solved for using an iterative method in Matlab.

**TABLE 4.10**  
Coefficients for species thermodynamic properties

Species	T range, K	$a_{11}$	$a_{12}$	$a_{13}$	$a_{14}$	$a_{15}$	$a_{16}$	$a_{17}$
CO <sub>2</sub>	1000-5000	0.44608(+1)	0.30982(-2)	-0.12393(-5)	0.22741(-9)	-0.15526(-13)	-0.48961(+5)	-0.98636(0)
	300-1000	0.24008(+1)	0.87351(-2)	-0.66071(-5)	0.20022(-8)	0.63274(-15)	-0.48378(+5)	0.96951(+1)
H <sub>2</sub> O	1000-5000	0.27168(+1)	0.29451(-2)	-0.80224(-6)	0.10227(-9)	-0.48472(-14)	-0.29906(+5)	0.66306(+1)
	300-1000	0.40701(+1)	-0.11084(-2)	0.41521(-5)	-0.29637(-8)	0.80702(-12)	-0.30280(+5)	-0.32270(0)
CO	1000-5000	0.29841(+1)	0.14891(-2)	-0.57900(-6)	0.10365(-9)	-0.69354(-14)	-0.14245(+5)	0.63479(+1)
	300-1000	0.37101(+1)	-0.16191(-2)	0.36924(-5)	-0.20320(-8)	0.23953(-12)	-0.14356(+5)	0.29555(+1)
H <sub>2</sub>	1000-5000	0.31002(+1)	0.51119(-3)	0.52644(-7)	-0.34910(-10)	0.36945(-14)	-0.87738(+3)	-0.19629(+1)
	300-1000	0.30574(+1)	0.26765(-2)	-0.58099(-5)	0.55210(-8)	-0.18123(-11)	-0.98890(+3)	-0.22997(+1)
O <sub>2</sub>	1000-5000	0.36220(+1)	0.73618(-3)	-0.19652(-6)	0.36202(-10)	-0.28946(-14)	-0.12020(+4)	0.36151(+1)
	300-1000	0.36256(+1)	-0.18782(-2)	0.70555(-5)	-0.67635(-8)	0.21556(-11)	-0.10475(+4)	0.43053(+1)
N <sub>2</sub>	1000-5000	0.28963(+1)	0.15155(-2)	-0.57235(-6)	0.99807(-10)	-0.65224(-14)	-0.90586(+3)	0.61615(+1)
	300-1000	0.36748(+1)	-0.12082(-2)	0.23240(-5)	-0.63218(-9)	-0.22577(-12)	-0.10612(+4)	0.23580(+1)
OH	1000-5000	0.29106(+1)	0.95932(-3)	-0.19442(-6)	0.13757(-10)	0.14225(-15)	0.39354(+4)	0.54423(+1)
NO	1000-5000	0.31890(+1)	0.13382(-2)	-0.52899(-6)	0.95919(-10)	-0.64848(-14)	0.98283(+4)	0.67458(+1)
O	1000-5000	0.25421(+1)	-0.27551(-4)	-0.31028(-8)	0.45511(-11)	-0.43681(-15)	0.29231(+5)	0.49203(+1)
H	1000-5000	0.25(+1)	0.0	0.0	0.0	0.0	0.25472(+5)	-0.46012(0)

Source: NASA Equilibrium Code.<sup>a</sup>

Figure 28: Polynomial Coefficients (Heywood 1988)

### 5.1.4 Correlation Plots

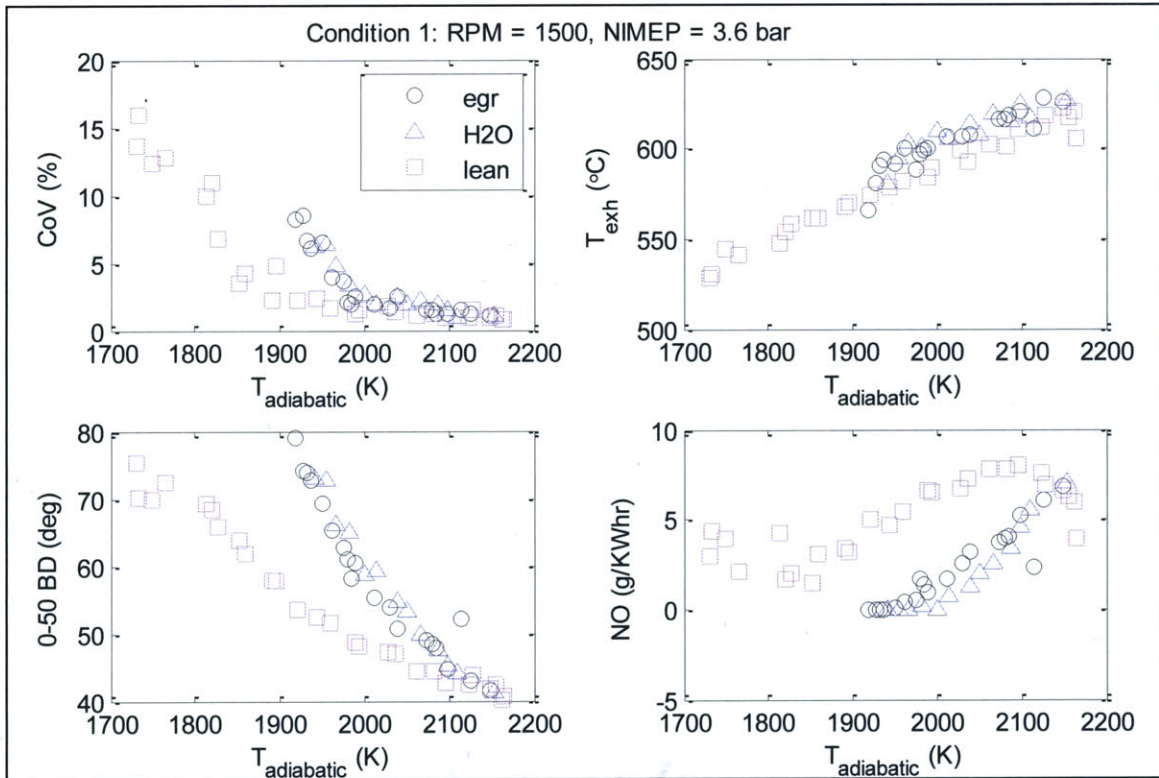


Figure 29: T-adiab correlations, Condition 1

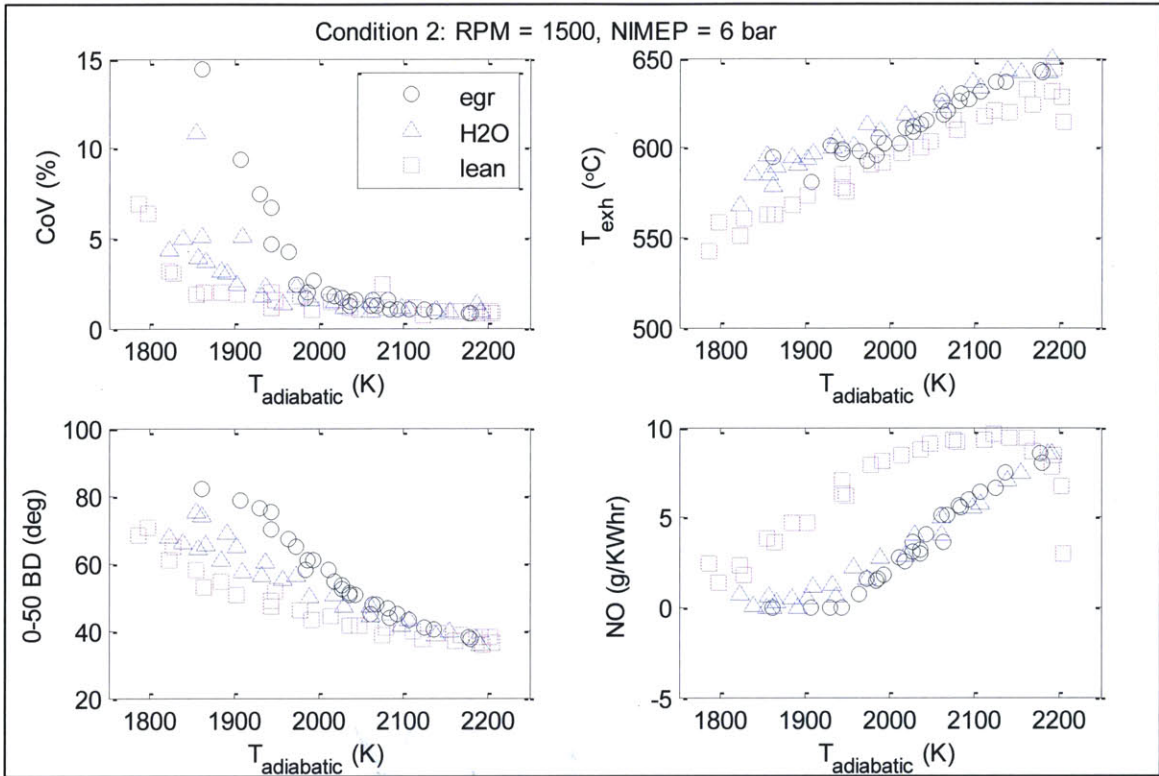


Figure 30: T-adiab correlations, Condition 2

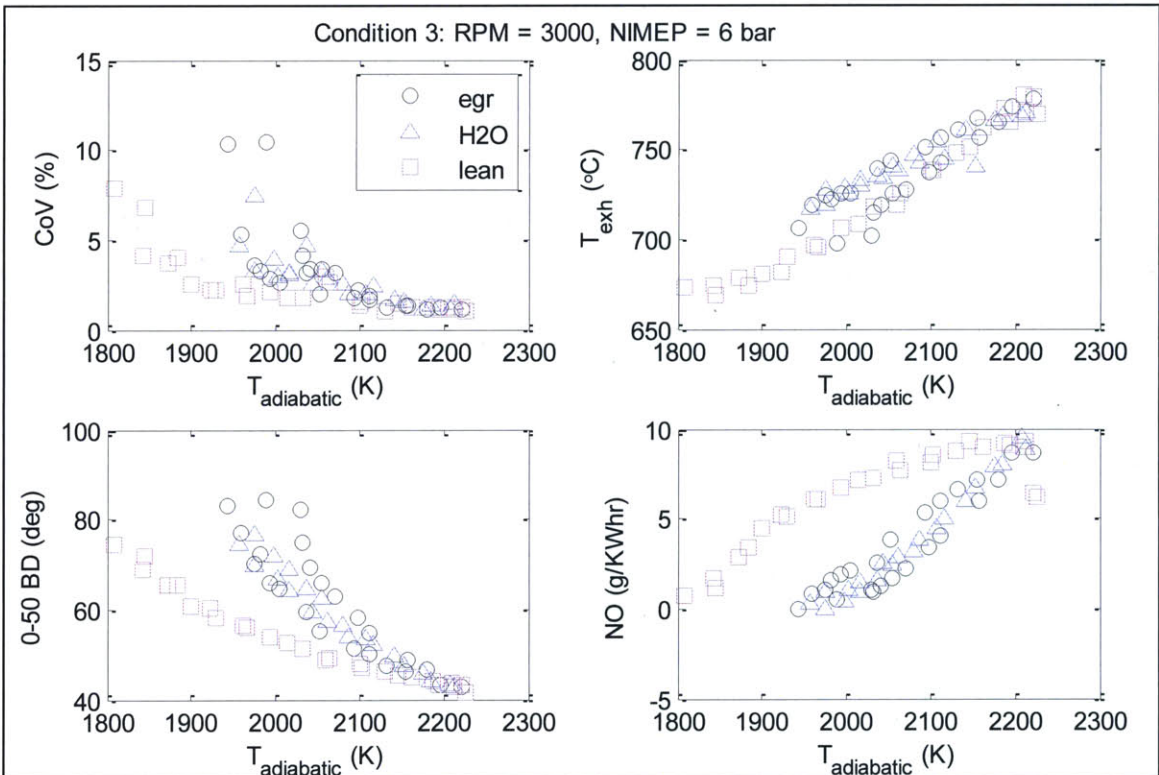


Figure 31: T-adiab correlations, Condition 3

As evident in Figure 29 through Figure 31, the use of adiabatic flame temperature as a metric has both pros and cons. For exhaust temperature, the three diluents correlate quite well. This can be reasonably expected given that flame temperature is the final temperature of the combustion products neglecting work and heat transfer. The only difference then is the work output and heat transfer effects. Work output is fixed as NIMEP is held constant for these experiments. Heat transfer losses are roughly proportional to the flame temperature if combustion phasing is ignored.

The other target outputs, however, did not correlate as well. The function forms are the same across the three diluents but parameters differ. For instance, CoV increased exponentially with a reduction in flame temperature; however this rate was different for each diluent. Horizontal shifts were also different. NOx production correlated well for EGR and water vapor cases but not for the lean case. This is understandable because oxygen plays a part in the nitric oxide formation process (Figure 3). The 0-50% burn duration also did not correlate well amongst the three diluents.

Since much of the burn duration and cycle-to-cycle variation of combustion have to do with the early flame development, the 0-50% burn duration and the CoV of NIMEP are thought to be related to the laminar flame speed,  $\delta_L$ , which correlates with the adiabatic flame temperature,  $T_a$ , see Equation 4. However, in our calculation, the adiabatic flame temperature,  $T_{ao}$ , is evaluated at a fixed reference condition  $T_o$  and  $P_o$ . The laminar flame speed at temperature  $T$  and pressure  $P$  may be expressed as:

$$S_L(T, P) = S_{Lo}(T_o, P_o) \cdot f(T, P)$$

Therefore  $T_{ao}$  would correlate to  $S_{Lo}$ , and encompass the effects of dilution on  $S_{Lo}$ . In the experiments, the CA50 is fixed, so the spark timing changes to maintain a fixed CA50. As a result, the  $T$  and  $P$  at the early flame development changes. Thus, while  $T_{ao}$  encompasses the dilution effects on  $S_{Lo}$ , the change of  $S_L(T, P)$  due to the  $T$  and  $P$  changes with the spark timing changes are not included. Hence using  $T_{ao}$  as a parameter does not collapse the data on CoV of NIMEP and 0-50% burn duration.

Because adiabatic flame temperature was not effecting in correlating the key combustion output, new metrics needed to be developed. Without tight correlations, it



would be very hard to use these methods in control strategy to predict outputs. The metric should also work when many diluents are used. It was seen that adiabatic flame temperature does not even have the ability to correlate single diluent cases. Thus it was not investigated further for interaction effects between EGR, water, and lean.

## 5.2 Ford EGR-Intake-Equivalent

Research efforts at Ford took an alternative approach to the adiabatic flame temperature metric. They developed what they termed the Wet EGR Intake Equivalent (EGR\_INT\_EQUIV\_WET). This is a lumped dilution parameter that accounts for each diluent individually. Each diluent is looked at as an inert gas that absorbs heat based upon its heat capacitance. They broke their study into two separate cases.

### 5.2.1 Humidity + EGR Equivalent

Determine total dilution:

$$\dot{m}_{TOTALDILUTION} = \dot{m}_{EGR} + \dot{m}_{HUMIDITY} \cdot \frac{C_p H_2O \text{ vapor}}{C_p EGR}$$

Equation 12

Approximation used for Cp ratio:

$$\frac{C_p H_2O \text{ vapor}}{C_p EGR} = 1.75$$

Equation 13

Calculate equivalent EGR:

$$EGR\_INT\_EQUIV\_WET = \frac{\dot{m}_{EGR-wet} + \dot{m}_{HUMIDITY} \cdot 1.75}{\dot{m}_{EGR-wet} + \dot{m}_{HUMIDITY} \cdot 1.75 + \dot{m}_{AIR}}$$

Equation 14

Using this metric as a means of correlating different quantities of diluents to engine output parameters, Ford achieved a high level of success.

### 5.2.2 Lean + EGR Equivalent

Similarly,

$$\dot{m}_{TOTALDILUTION} = \dot{m}_{EGR} + \dot{m}_{HUMIDITY} \cdot \frac{C_p \text{ Air}}{C_p \text{ EGR}}$$

Equation 15

$$\frac{C_p \text{ Air}}{C_p \text{ EGR}} = .92$$

Equation 16

$$EGR\_INT\_EQUIV\_WET = \frac{\dot{m}_{EGR-wet} + \dot{m}_{EXCESS-AIR} \cdot .92}{\dot{m}_{EGR-wet} + \dot{m}_{EXCESS-AIR} \cdot .92 + \dot{m}_{AIR}}$$

Equation 17

### 5.2.3 Overall Equivalent

Combining diluents,

$$EGR\_INT\_EQUIV\_WET = \frac{\dot{m}_{EGR-wet} + \dot{m}_{EXCESS-AIR} \cdot .92 + \dot{m}_{HUMIDITY} \cdot 1.75}{\dot{m}_{EGR-wet} + \dot{m}_{EXCESS-AIR} \cdot .92 + \dot{m}_{HUMIDITY} \cdot 1.75 + \dot{m}_{AIR}}$$

Equation 18

### 5.2.3 Correlation Plots

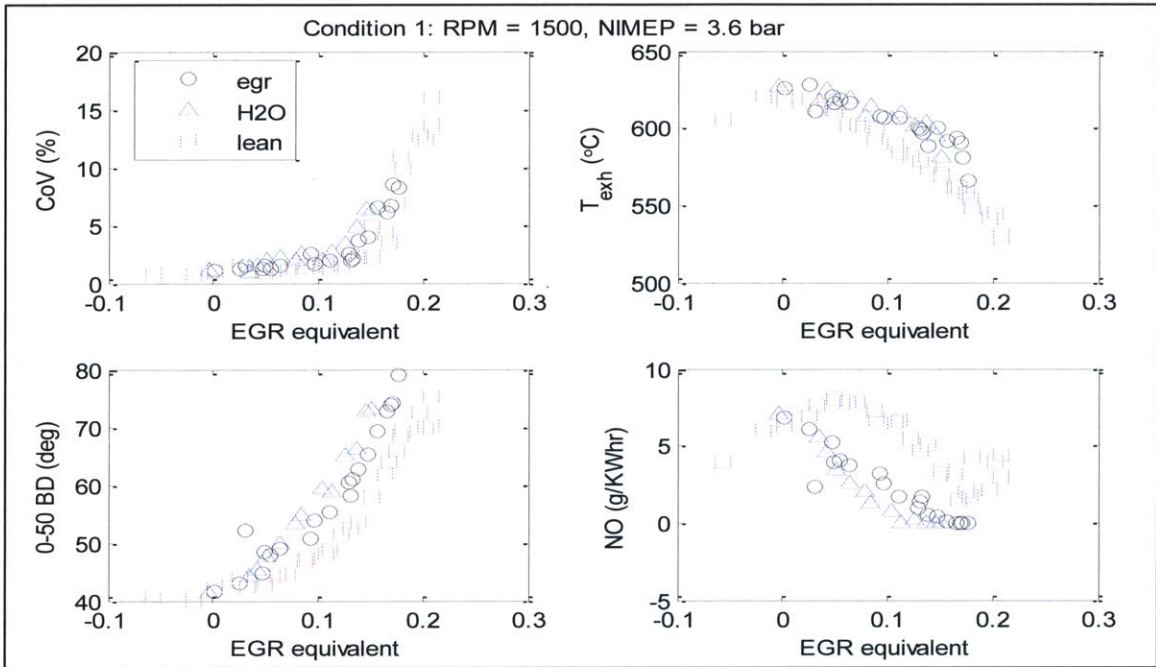


Figure 32: EGR equivalent correlations, Condition 1

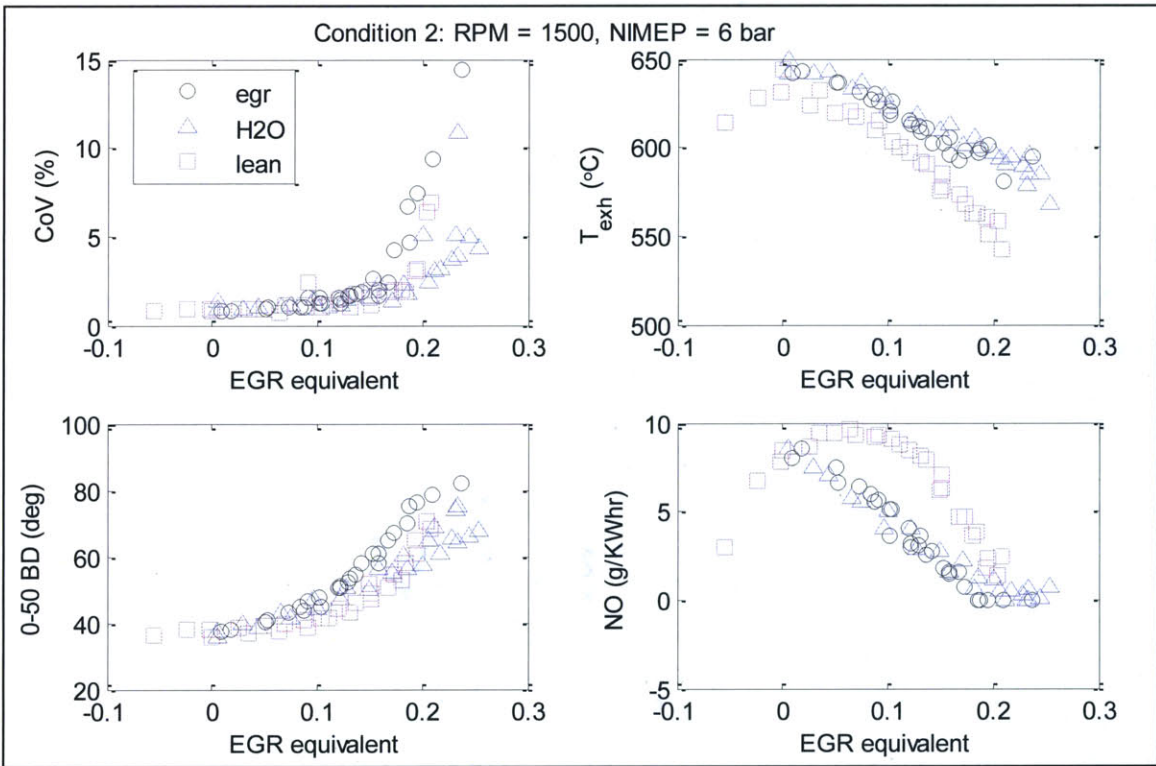


Figure 33: EGR equivalent correlations, Condition 2

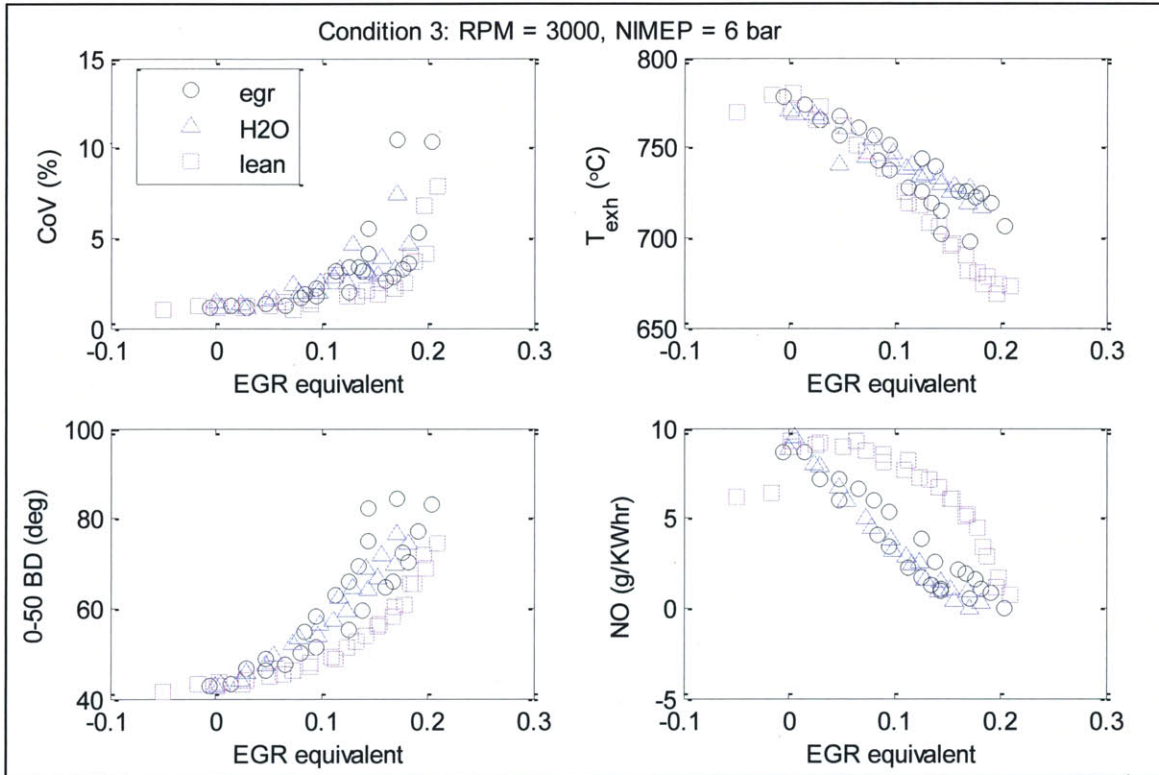


Figure 34: EGR equivalent correlations, Condition 3

As evident in the plots show in Figure 32 through Figure 34, the Ford EGR equivalent correlates the engine output data better than the adiabatic flame temperature metric. Correlation is quite well for the exhaust temperatures at low dilution, CoV, and the 0-50 burn duration. Correlation is also not expected for the NOx lean sweep due to excess oxygen. Nonetheless, the level of correlation achieved does not compare to the high level that Ford was able to achieve. The results shown do show promise. Many of the dilution trends shown in the plots differ only by horizontal stretching/shrinking. This leads the way into the third metric attempted. The coefficients such as .92 and 1.75 in Equation 18 were modified to attain better correlations and thus be more useful in control strategy.

### 5.3 Regression of Diluents

#### 5.3.1 Methodology

This third correlation metric was attempted using a linear combination of diluents. It is a purely empirical method, but one that resulted in the best correlation results. The metric is defined for each engine output as shown below:

$$CoV_{eqv} = egr + a_1 * h_{2o} + a_2 * (\lambda - 1)$$

Equation 19

$$Texh_{eqv} = egr + b_1 * h_{2o} + b_2 * (\lambda - 1)$$

Equation 20

$$BD0_{50_{eqv}} = egr + c_1 * h_{2o} + c_2 * (\lambda - 1)$$

Equation 21

$$NO_{eqv} = egr + d_1 * h_{2o} + d_2 * (\lambda - d_3)$$

Equation 22

Where

$$egr \equiv \frac{m_{egr}}{m_{air} + m_{egr}} \text{ and } h_{2o} \equiv \frac{m_{h2o}}{m_{air}}$$

For each target output quantity the coefficients were chosen to minimize deviation from the general trend. These coefficients were then averaged for the three cases. (The three cases refer to speed and NIMEP of 1500 rpm, 3.6 bar; 1500 rpm, 6 bar; and 3000 rpm, 6 bar.) These averages were then used to correlate the data shown in the plots in the following section.

COV_eqv=egr+a1*h2o+a2*(lambda-1)			AVERAGES	
	a1	a2		
Case 1	1.4	0.5	a1	1.36667
Case 2	1.3	0.5	a2	0.48333
Case 3	1.4	0.45		
Texh_eqv=egr+a1*h2o+{a2*(lambda-1) if lambda!=1}				
	a1	a2		

Case 1	1.4	0.95			a1	1.33333
Case 2	1.3	1			a2	0.96
Case 3	1.3	0.93				
$BD0-50_{eqv} = egr + a1 \cdot h2o + a2 \cdot (\lambda - 1)$						
	a1	a2				
Case 1	1.55	0.5			a1	1.36667
Case 2	1.4	0.45			a2	0.46667
Case 3	1.45	0.45				
$NO_{eqv} = egr + a1 \cdot h2o + a2 \cdot (\lambda - a3)$						
	a1	a2	a3			
Case 1	1.6	0.6	1.15		a1	1.5
Case 2	1.45	0.8	1.2		a2	0.66667
Case 3	1.45	0.6	1.15		a3	1.16667

Table 12: Linear combination coefficients

### 5.3.2 Correlation Plots

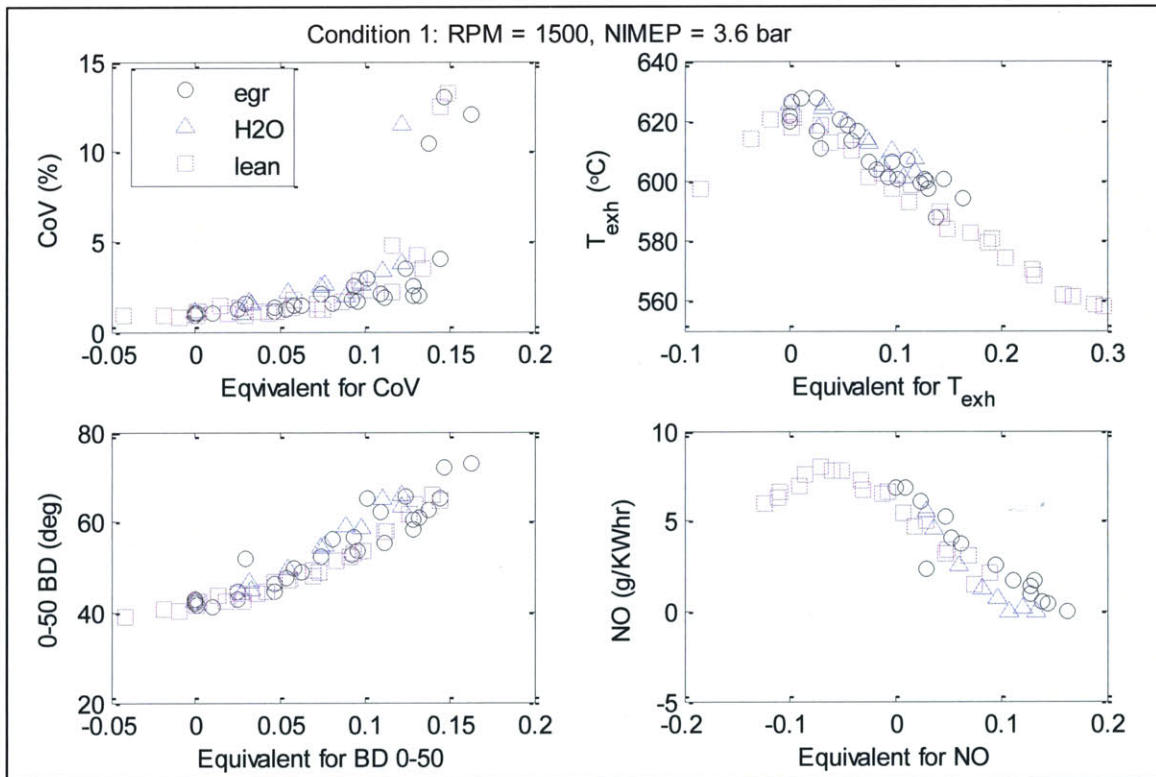


Figure 35: Linear combination equivalent correlations, Condition 1

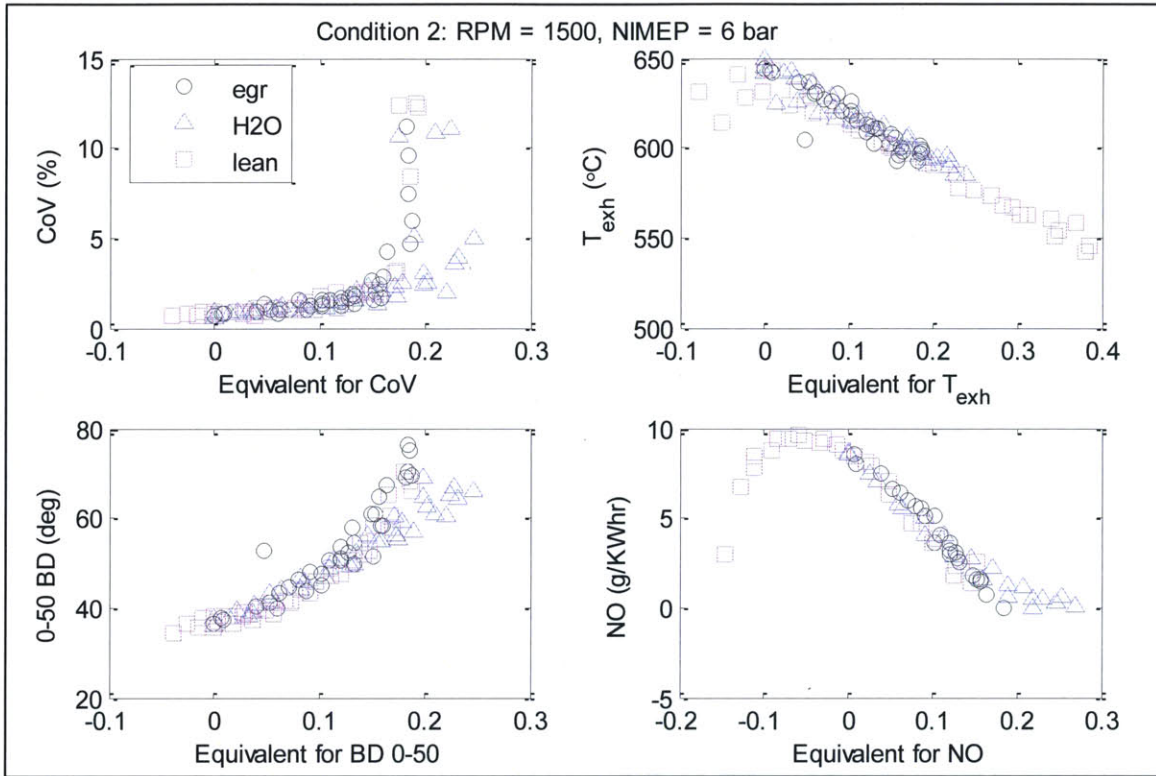


Figure 36: Linear combination equivalent correlations, Condition 2

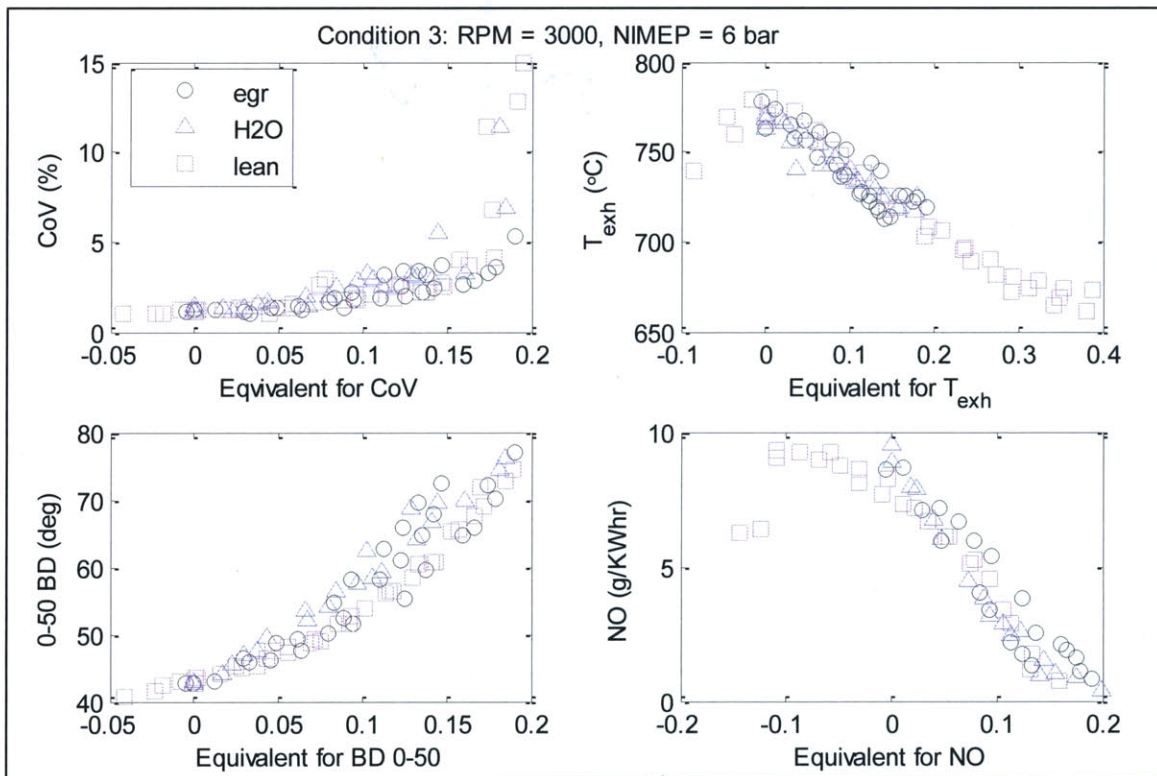


Figure 37: Linear combination equivalent correlations, Condition 3

The correlations provided using this metric were very promising. Of the three metrics attempted, this correlation metric yielded the best results. This does not necessarily come as a surprise. It is a purely empirical method. A, b, c, and d coefficients were chosen to achieve the tightest fits. This implies that key combustion outputs can be predicted knowing the quantities of each diluent. Another great benefit of this fit over the others is evident with the lean case of NO<sub>x</sub>. This method accounts for fact that NO<sub>x</sub> peaks slightly lean via the addition of a third parameter,  $d_3$ . This effectively shifts the curve to the right. It is also worth noting that the coefficients  $a_1$  and  $a_2$  are approximately the same for the  $CV_{eqv}$  and  $BD0-50_{eqv}$ . Thus the CoV and 0-50% burn duration react similarly to dilution.

One problem that did become evident is correlating CoV at high dilution. Once dilution hits a certain threshold, CoV increases very rapidly. Figure 36 illustrates this most vividly for CoV in the case of low speed, high load. This makes choosing the parameters of Equation 19 through Equation 22 difficult. For cases such as these, it was decided to focus a larger effort on correlating the data in the low to mid-range dilution cases. This was decided because in normal engine operating conditions, high dilution/high CoV is undesirable anyways.



## 5.4 Interaction Effects

As a final part of this project, interaction effects were studied for the various diluents. For this, data was used from dual parameters sweeps described in section 2.3.1 Engine Experiments. Because the linear combination of diluents yielded the best results for the single diluent sweeps, this method was attempted with the dual diluent sweeps. To correlate the data, the same coefficients from Table 12 were used. Correlation results from this study were very promising. For instance, Figure 38 shows an EGR and water vapor interaction for the low speed, high load case. Plots for all nine cases are provided in Appendix , Figure 40 through Figure 48.

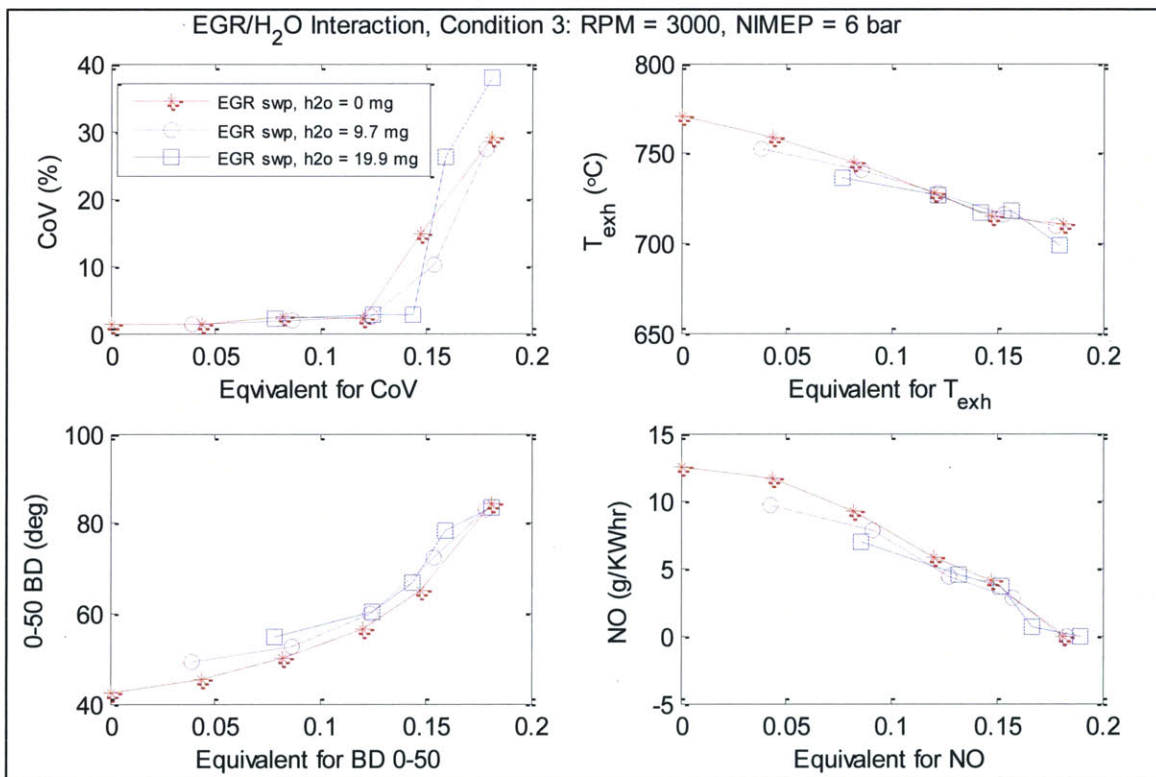


Figure 38: EGR – H<sub>2</sub>O interaction plot

Results such as this indicate that multiple diluents can be correlated without the addition of variables to the correlation metric equations (Equation 19 to Equation 22). Diluents appear to add quite linearly. This is especially true for exhaust temperature, CoV, and 0-50 burn duration. The output that did not correlate quite as well was NOx. The variation is potentially caused by variance in the third NOx parameter for the lean

contribution of Equation 22. This deduction is drawn because NO<sub>x</sub> correlates very well for the EGR – H<sub>2</sub>O interaction cases such as that of Figure 36. It does not correlate as well for the H<sub>2</sub>O – Lean cases such as that shown below in

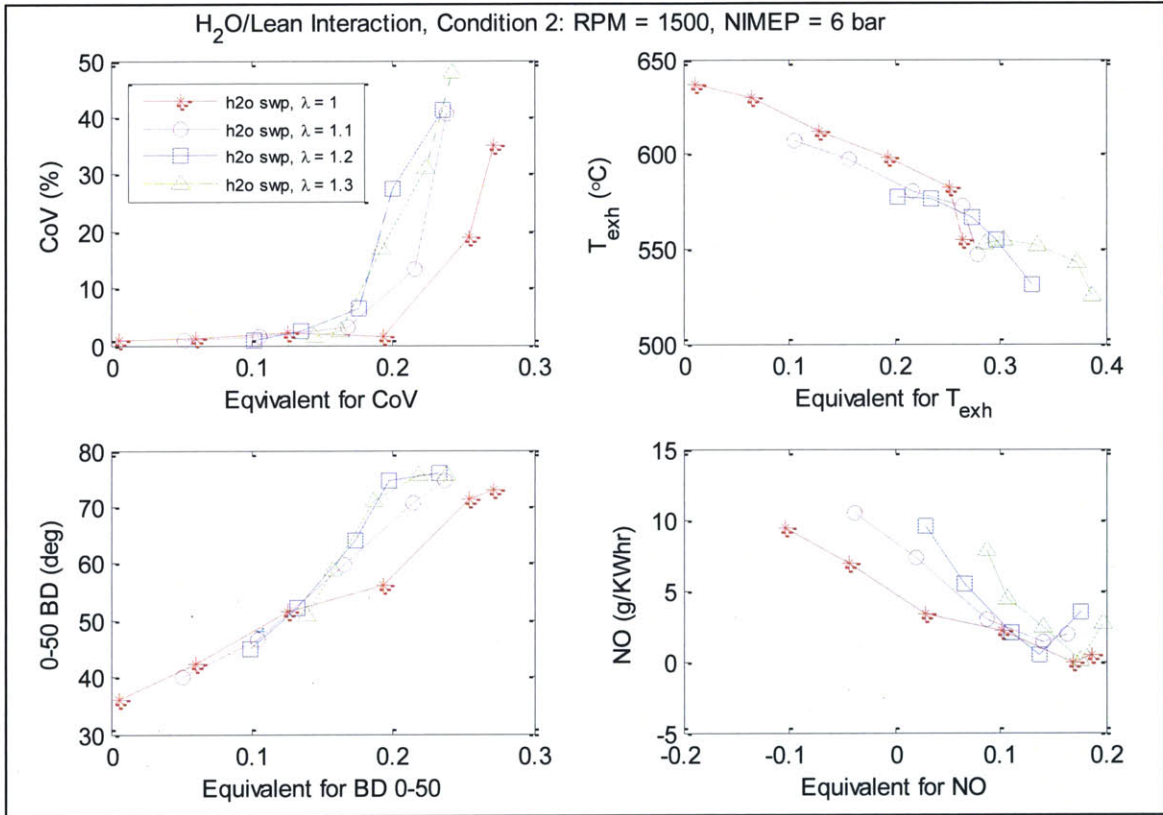


Figure 39: H<sub>2</sub>O – Lean

## CHAPTER 6 – CONCLUSIONS

The purpose of this research was to translate the dilution tolerance of an engine for different diluents. The objective was to relate combustion inputs such as the quantities of air, EGR, and water vapor to combustion outputs such as CoV, NO<sub>x</sub>, exhaust temperature, and combustion phasing. Results from this study can then be used at Ford in developing control strategies for modern spark ignition engines. In order for these results to be useful, it was necessary to develop a correlation which worked at a wide range of operating conditions. For the purpose of this study, three operating conditions were used ranging from low speed, low load to high speed, high load. A variety of metrics were attempted to achieve the goals of the project.

Initially, it was believed that combustion outputs could be reasonably be correlated using a fundamental scientific metric. Thus, the first metric chosen was adiabatic flame temperature. This is a highly comprehensive property that encompasses a large amount of thermodynamic phenomena. Enthalpy and combustion potential is embedded in this term. Despite this intuitive rationale, adiabatic flame temperature proved to be unsuccessful in predicting the key combustion outputs. Flame temperature only proved effective in correlating exhaust temperature across different diluents. It was also evident very quickly that adiabatic flame temperature alone would be insufficient to predict NO<sub>x</sub> formation in the lean condition. This is because NO<sub>x</sub> peaks in a slightly lean condition around lambda of 1.1. The other drawback using flame temperature was that it was quite computationally intensive. For each test, an iterative solution was performed to equate the enthalpy of the products to the enthalpy of the reactants.

As an alternative to adiabatic flame temperature which proved ineffective in predicting engine output quantities, the Ford EGR-intake equivalent was examined. This was a methodology developed by Ford as a similar means of predicting combustion outputs. The underlying science of this metric is similar to flame temperature. The metric assumed a specific heat for each diluent which contribute to the overall dilution. Overall, this method was much less computationally intensive. It was able to be simplified down to a linear equation. The results of this were significantly better than that for adiabatic flame temperature. Nonetheless, they did not produce tight correlations

that could be useful in control strategies. It was concluded that too much variation still existed amongst the diluents. It was also found that the results differed from that of Ford. Ford was able to attain very tight correlations unlike this research.

Finally, a third method was attempted to achieve the goals of this research. It was concluded that this method had the best results. This method consisted of generating a diluent equivalent for each combustion output (exhaust temperature, CoV, NO<sub>x</sub>, and combustion phasing). Each diluent fraction was multiplied by an empirical parameter based on experimental data. These parameters were averaged for all operating conditions. The pitfall of this metric is that it relies only on empirical data and not underlying combustion physics. It is also conceivable that these parameters would vary depending on depending on the engine. This would lead to the pursuit of less aggressive control strategies reducing the impact of this research.

Overall, this research set out what it intended to do which was translate the dilution tolerance for a gasoline SI engine. Many metrics were attempted to correlate the real engine data across the three different diluents studied. Three metrics were presented in this work. Many more were attempted over the course of this research. Overall, the method which achieved the best ability to predict combustion outputs was the linear combination of diluents. This research should lead to the successful implementation of control strategies utilizing multiple dilution technologies.

## REFERENCES

- Affelt, Scott. *Reduce CO2 Emissions and Boost Generation Efficiency*. September 1, 2011. <http://www.power-eng.com/articles/print/volume-115/issue-7/features/reduce-co2-emissions-and-boost-generation-efficiency.html> (accessed February 28, 2013).
- Alger, T., Gingrich, J., Mangold, B. "The Effect of Hydrogen Enrichment on EGR Tolerance in Spark Ignited Engines." *SAE 2007-01-0475*, 2007.
- Ayala, F., Gerty, M., Heywood, J. "Effects of Combustion Phasing, Relative Air-Fuel Ratio, Compression Ratio, and Load on SI Engine Efficiency." *SAE 2006-01-0229*, 2006.
- Ayala, F., Heywood, J.B. "Lean SI Engines: the Role of Combustion Variability in Defining Lean Limits." *SAE 2007-24-0030*, 2007.
- Benson, G. *Wikipedia*. August 1, 2004. <http://en.wikipedia.org/wiki/File:Dewpoint.jpg> (accessed February 27, 2013).
- Clean Air and You*. n.d. [http://www.agcocorp.com/e3/clean\\_air\\_and\\_you.aspx](http://www.agcocorp.com/e3/clean_air_and_you.aspx) (accessed January 20, 2013).
- Depcik, Christopher. *Adiabatic Flame Temperature*. March 25, 2013. <http://en.wikipedia.org/wiki/File:Urup.jpg> (accessed March 10, 2013).
- DiamlerChrysler. *Service Manual 2.4L Engine*. 2003.
- Feng, A., DeCicco, J. "Trends in Technical Efficiency Trade-Offs for the U.S. Light Vehicle Fleet." *SAE 2007-01-1325*, 2007.
- Gordon, S. McBride, B.J. "Computer Program for Calculating Complex Chemical Equilibria, Rocket Performance, Incident and Reflected Shocks, and Chapman-Jouguet Detonations." *NASA*, 1976.
- Gordon, S., McBride, B.J. "Computer Program for the Calculation of Complex Chemical Equilibrium Composition." *NASA Reference Publication 1311*, 1994.

- HaltermannSolutions. "HF-437 Certificate of Analysis." 2012.
- Heywood, J.B. *Internal Combustion Engine Fundamentals*. New York: McGraw Hill, 1988.
- Horiba. *MEXA-720 Service Manual*. 2012.
- Lang, K. "Reducing Cold Start Hydrocarbon Emissions from Port Fuel Injected Spark Ignition Engines with Improved Management of Hardware and Controls." *Doctoral Thesis*, MIT 2006.
- Mechadyne International. *Part Load Pumping Losses in an SI Engine*. 2012. <http://www.mechadyne-int.com/vva-reference/part-load-pumping-losses-si-engine> (accessed April 12, 2013).
- Mendera, K., Spyra, A., Smereka, M. "Mass Fraction Burned Analysis." *Journal of KONES internal Combustion Engines*, 2002.
- Pischinger, Stefan. "Effects of Spark Plug Design Parameters on Ignition and Flame Development in an SI-Engine." *MIT Ph.D. Thesis*, 1985.
- Pope, Bates, Raizenne. "Health effects of particulate air pollution: time for reassessment?" *Environ Health Perspect*, 1995: 472-480.
- Price, P., Stone, R. "Cold Start Particulate Emissions from a Second Generation DI Gasoline Engine." *SAE*, 2007.
- Tabor, Joe. *United States Humidity Zones*. November 16, 2001. <http://ag.arizona.edu/oals/soils/surveys/states.html> (accessed January 10, 2013).

## APPENDIX A

### Standard Operating Procedure

No.	Action
<b>Turning on cooling water, power, electrical (inside test cell)</b>	
1	Turn on trench fan and city water pump (green and yellow lights). Located on wall between Kevin's and Sang Wen's test cell. Probably on but ask if you don't know.
2	Turn on breakers. (Located in the box at the rear of the test cell - again probably on)
3	Turn on Box #1 and #4 on the left side of the test cell. Box #1 controls dyno motor (480 volts – lots of power). Box 4 controls the dyno controller (less power)
4	Open city water valve (ensure dyno and engine valves are also open- halfway is recommended for both). Adjust main valve to get between 20 and 40 psi on the indicator.
5	Check engine oil level. Read the dipstick to ensure proper level.
<b>Turning on Electronics (outside test cell)</b>	
6	Turn on MASTER switch on the control panel.
7	Turn on ENGINE COOLANT PUMP & PID CTRL switch on the control panel. This is the pump right side of the dyno near the large coolant tank covered in black foam. Ensure sufficient coolant level. There is a tube on the side that shows you.
8	Set Engine coolant temperature on PID, and set to 'Run' (e.g. 85°C). May need to consult test binder/temperature controller if you can't figure it out or ask Professor Cheng. Note: This process takes a while to equilibriate – if you are running at a specific temperature, you will have to do this well in advance of others steps.
9	Turn on DYNO COOL PUMP switch on the control panel. This is the pump on the left side of the dyno. Ensures the dyno can dissipate energy as heat.
10	Turn on FUEL PUMP switch on the control panel. This turns on the pump beneath the silver gas tank. The pressure indicated should read between 40 and 60 psi. Also, make sure to maintain a healthy amount of fuel in the tank so as not to run out in the middle of a test.
11	Turn on CKT#6 switch on the control panel. This is a switch to the power strip in the middle of the test cell on the shelf. Plugged into this are devices such as the amplifier for the pressure transducer, horiba lambda sensor, CA & BDC box, and ignition/injection drivers.
12	Put Horiba meter on top of the engine into Lambda mode by pressing M. Should read 9.999.
<b>Starting the engine (not firing... yet)</b>	
13	Press the green START button on the control panel (DYNO START/STOP). This starts up the motor of the dyno. Wait 30 seconds for speed to stabilize
14	Turn on the CONTROLLER ON/OFF button on the left panel of the control panel. The button should light up. Also ensure the dyno is in duo or motoring mode (white buttons on bottom)
15	Adjust RPM to desired level. Recommendation- start at 1500 rpm.

16	Press the DYNOMOMETER CLUTCH button to the left of the CONTROLLER ON/OFF button. This engages the clutch and the engine should start rotating. If not, diagnose or consult Professor Cheng.
17	Set engine to desired load. This is controlled by the throttle. On my system this is the ball valve about the engine near the blue tank. The black MAP sensor above the engine displays the intake pressure in bar. Set to .5 to .6 bar. There are also open and close buttons on the front panel which allow for finer adjustment via the flow bypass.
<b>Starting Labview</b>	
18	Log onto master computer (black dell) under the Sloan Lab username.
19	Open Labview program: C:\Documents and Settings\Sloan Lab\Desktop\DISI LabView\Front panel_Troy.vi on the master computer. Shortcut on desktop
20	Run the program (arrow in upper left). Values should start to update
21	Put charge amplifier from the cylinder pressure transducer into run mode. This should give you a pressure trace on the front panel. If the pressure rise is on the right half of the graph, flip the phase select toggle on the CA & BDC CIRCUIT box above the engine.
22	Get ready for data acquisition (e.g. datasheet, new folder, etc.). Select data path on LabVIEW front panel for which you want data to save.
<b>Start firing engine</b>	
23	Restart slave computer (old white dell) in ms-dos mode. Computer may prompt you to return to normal mode – enter N. Change director to C with command “cd \c”
24	Start master_b on Master computer (C:\C\master_b\Release) or shortcut from desktop. Input rpm (1500), then lambda (1), eoi (500), spark (150). Think these values through the first time.
25	Make sure injection switch #1 near the monitor is set to the on position and the terminate toggle is in the bottom position. Start single_a on Slave computer. Input initial injection duration (6000).
26	Fire the engine for 4-5 minutes for fuel purge and stabilization
27	Set MAP to operating point for experiment by opening and closing throttle. To adjust speed restart master_b and single_a and use desired values
28	Conduct experiments and record data



### EGR Control

No.	Action
1	Make sure ball valve next to EGR valve is open
2	Plug in control box lying on desk outside test cell.
3	Plug BNC- 2 prong output into voltmeter
4	Use course and fine adjusters to achieve desired EGR level (higher voltage means more EGR is being allowed through the valve)

### Water Injection Control

No.	Action
<b>Inside the test cell</b>	
1	Fill water tank with distilled water. Tank is located next to gas tank.
2	Pressurize tank using the tank of nitrogen located along the right wall of the test cell. Water flow rate is a function of pressure- see calibration curves when choosing the psi.
3	Move 3-way valve to allow water from the tank to be injected. When done, rotate back so that nitrogen flows to injector. This prevents rusting of the injector.
<b>Outside test cell</b>	
4	Power on the pulse generator
5	Adjust pulsewidth to desired level. 1 ms is a good starting point
6	Use oscilloscope to verify waveform
7	Flip injection switch #2 to ON position

### Shutdown Procedure – Troy Niekamp

No.	Action
1	Set dyno speed back to 1500 rpm
2	Terminate firing programs and set the injector safety switches to OFF
3	Reset MAP to 0.5 bar
4	Motor the engine for 2-3 minutes for cool-down
5	Disengage the clutch, let engine stop
6	Turn off the dyno controller
7	Press DYNO STOP (red button)
8	Allow dyno cooling to continue for 1-2 minutes
9	Turn off dyno coolant pump, fuel pump ,and CKT#6
10	Allow engine cooling to continue for 2-3 minutes
11	Turn off engine coolant pump and PID
12	Turn off city water valve
13	Turn off Boxes #1 and #4 if you are going to be working on engine
14	Turn off city water and trench fan (if applicable)
15	Lights out and lock up the lab

## APPENDIX B

### Fuel Specifications

**HALTERMANN**

**PRODUCT: EPA TIER II EEE  
FEDERAL  
REGISTER**

**PRODUCT  
CODE: HF437**

TEST	METHO D	UNITS	FED Specs		HALTERMANN Specs			Typical Results
			MIN	MAX	MIN	Target	MAX	
Distillation - IBP	ASTM D86	°F	75	95	75		95	89
5%		°F						117
10%		°F	120	135	120		135	131
20%		°F						154
30%		°F						181
40%		°F						209
50%		°F	200	230	200		230	224
60%		°F						234
70%		°F						244
80%		°F						267
90%		°F	305	325	305		325	321
95%		°F						335
Distillation - EP		°F		415			415	402
Recovery		vol %				Report		98.0
Residue		vol %				Report		1.0
Loss		vol %				Report		1.0
Gravity	ASTM D4052	°API	58.7	61.2	58.7		61.2	58.9
Density	ASTM D4052	kg/l			0.734		0.744	0.743
Reid Vapor Pressure	ASTM D323	psi	8.7	9.2	8.7		9.2	9.1
Reid Vapor Pressure	ASTM D5191	psi				Report		9.00
Carbon	ASTM D3343	wt fraction				Report		0.8664
Carbon	ASTM E191	wt fraction				Report		0.8641

Hydrogen	ASTM E191	wt fraction				Report		0.1309
Hydrogen/Carbon ratio	ASTM E191	mole/mole				Report		1.805
Oxygen	ASTM D4815	wt %					0.05	<0.05
Sulfur	ASTM D5453	wt%	0.0015	0.0080	0.0025		0.0035	0.0029
Lead	ASTM D3237	g/gal		0.05			0.01	<0.01
Phosphorous	ASTM D3231	g/gal		0.005			0.005	<0.0008
Composition, aromatics	ASTM D1319	vol %		35.0			35.0	30.7
Composition, olefins	ASTM D1319	vol %		10.0			10.0	0.5
Composition, saturates	ASTM D1319	vol %				Report		68.8
Benzene	ASTM D3606	vol%				Report		0.1
Particulate matter	ASTM D5452	mg/l					1	0.6
Oxidation Stability	ASTM D525	minutes			240			>1000
Copper Corrosion	ASTM D130						1	1
Gum content, washed	ASTM D381	mg/100mls					5	<1
Fuel Economy Numerator/C Density	ASTM E191				2401		2441	2433
C Factor	ASTM E191					Report		0.9992
Research Octane Number	ASTM D2699		93.0		96.0			97.4
Motor Octane Number	ASTM D2700					Report		89.0
Sensitivity			7.5		7.5			8.4
Net Heating Value, btu/lb	ASTM D3338	btu/lb				Report		18450
Net Heating Value, btu/lb	ASTM D240	btu/lb				Report		18435
Color	VISUAL					Report		CLEAR

# Appendix C

## Interaction Plots

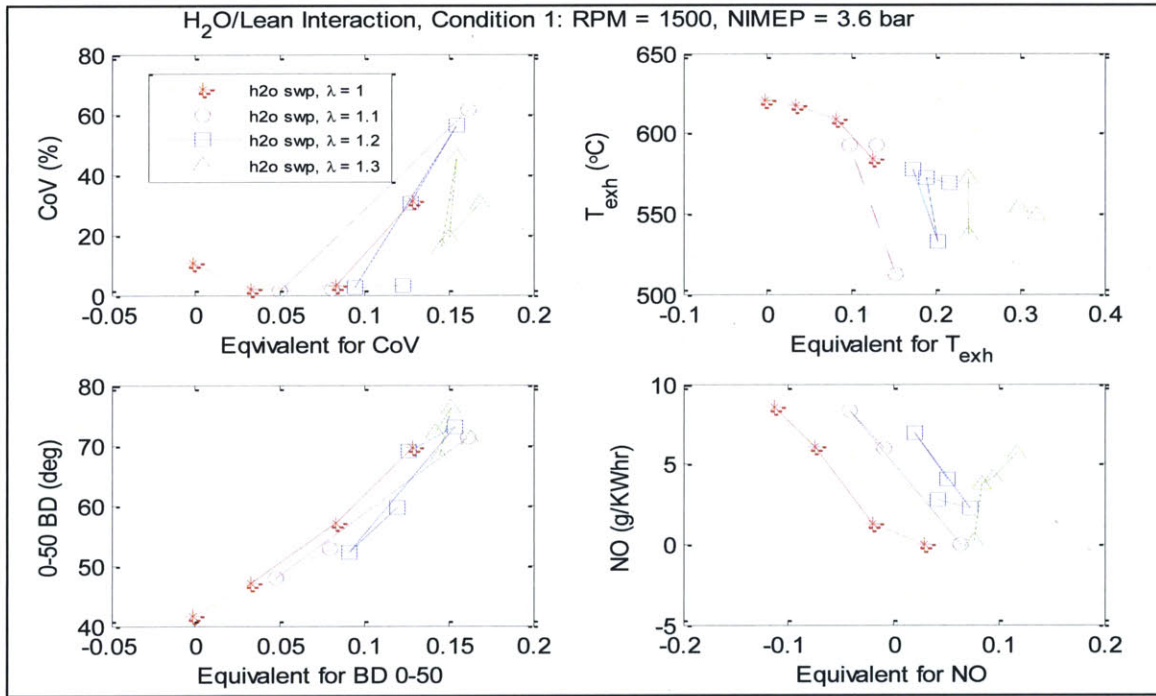


Figure 40: H<sub>2</sub>O – Lean Interaction, Condition 1

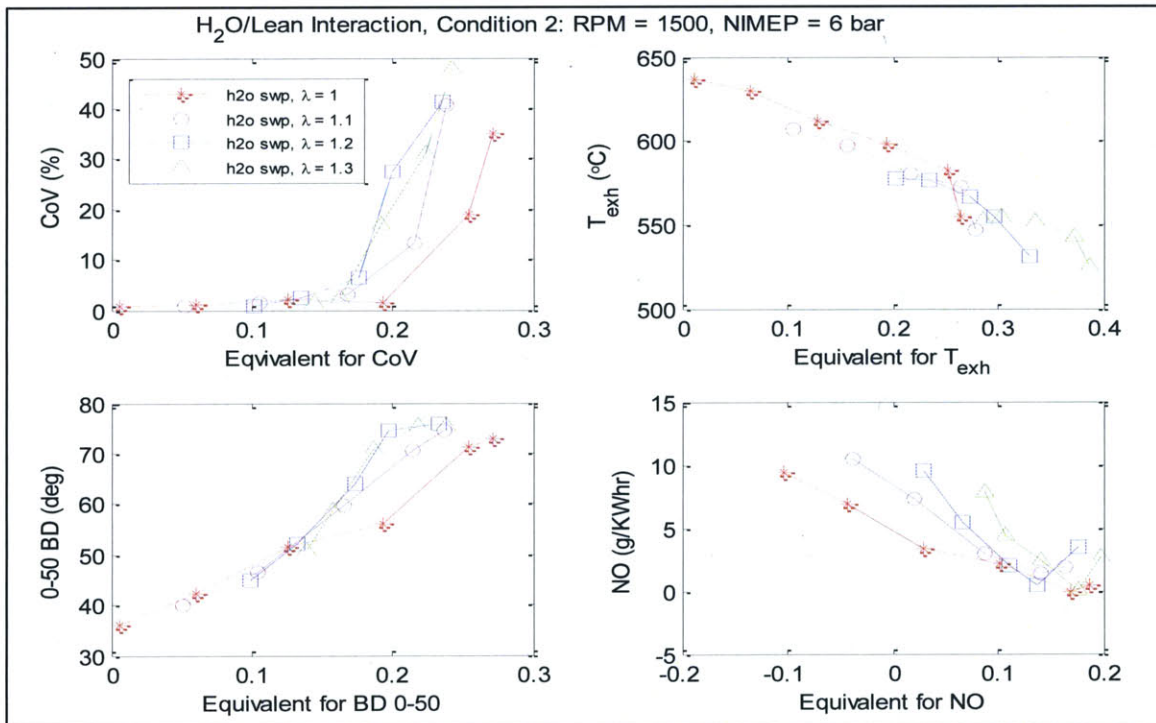
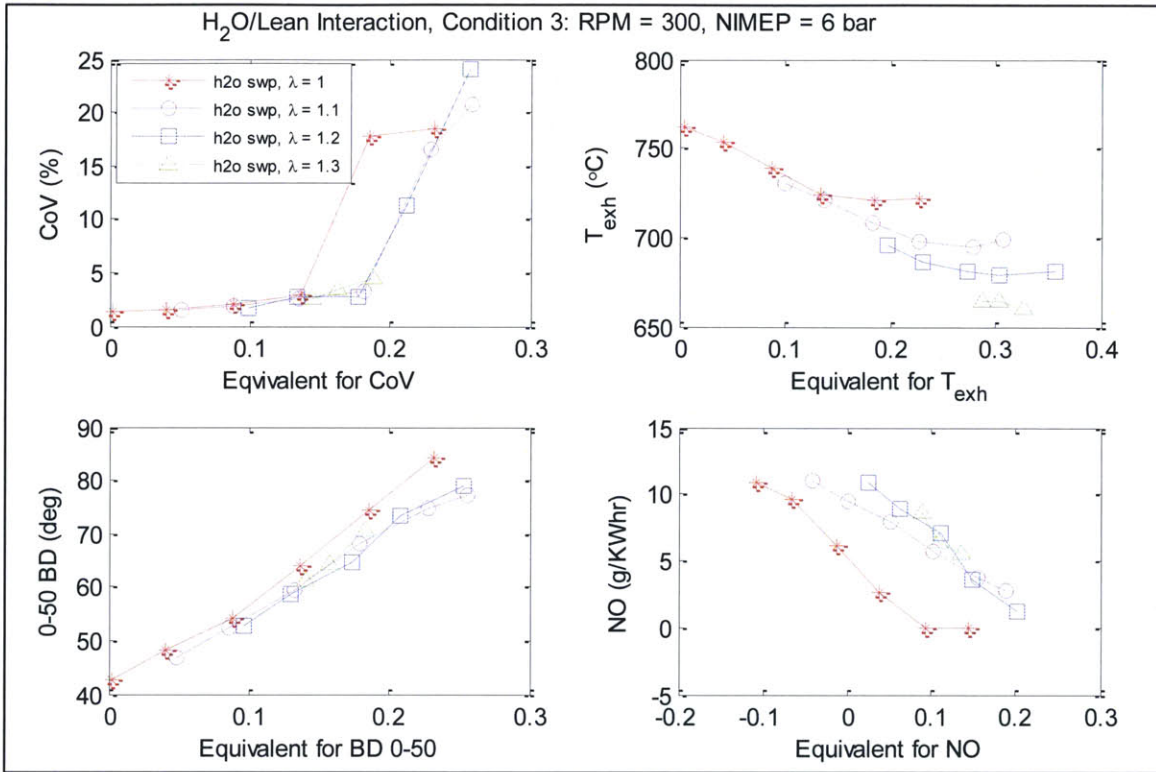
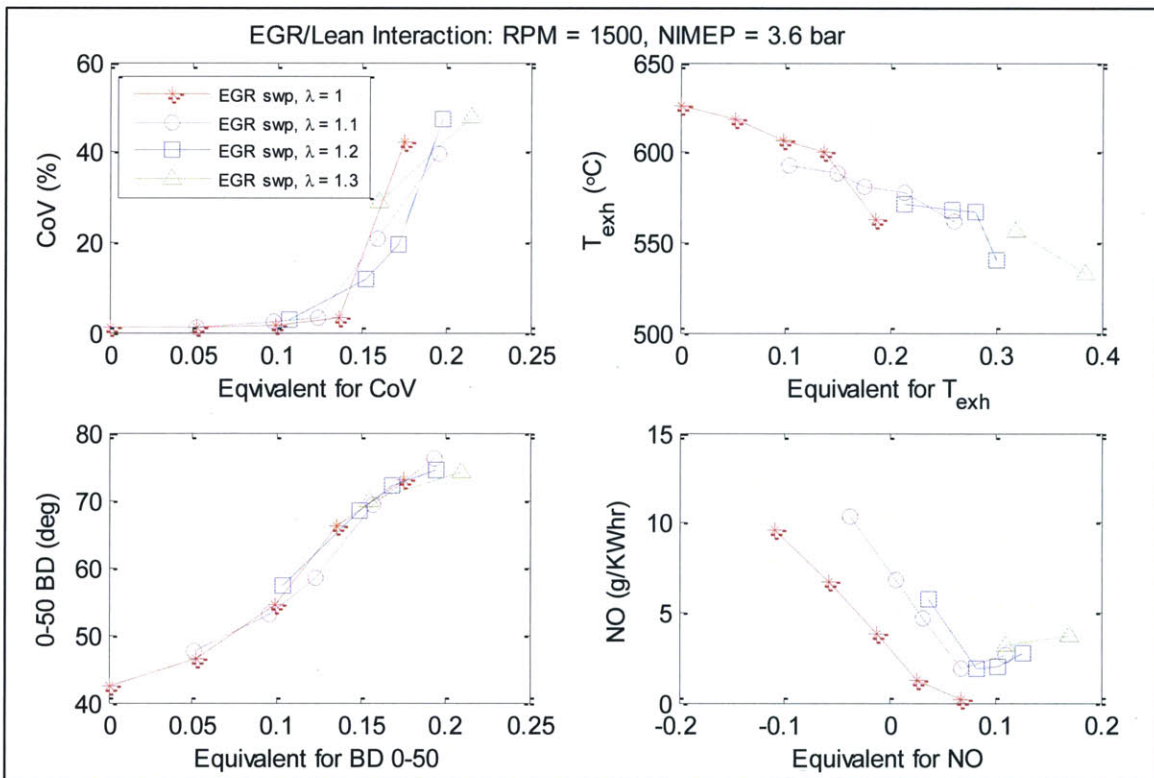


Figure 41: H<sub>2</sub>O – Lean Interaction, Condition 2



**Figure 42: H<sub>2</sub>O – Lean Interaction, Condition 3**



**Figure 43: EGR – Lean Interaction, Condition 1**

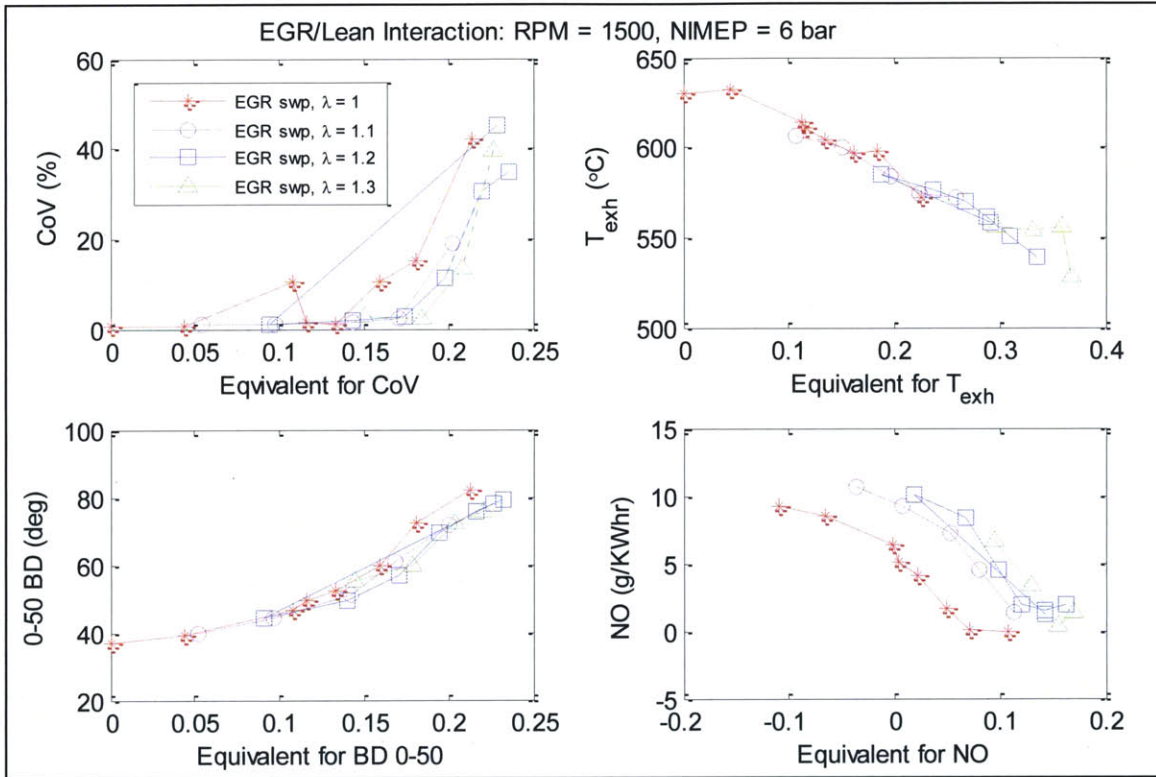


Figure 44: EGR – Lean Interaction, Condition 2

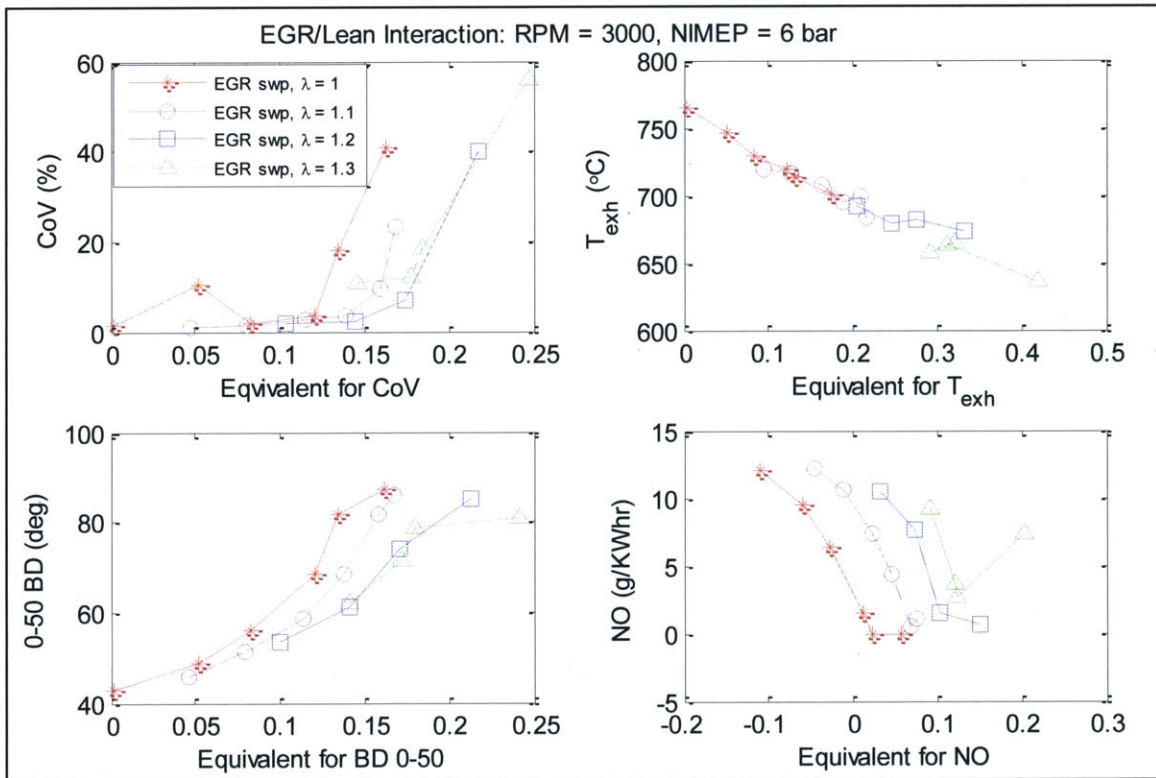
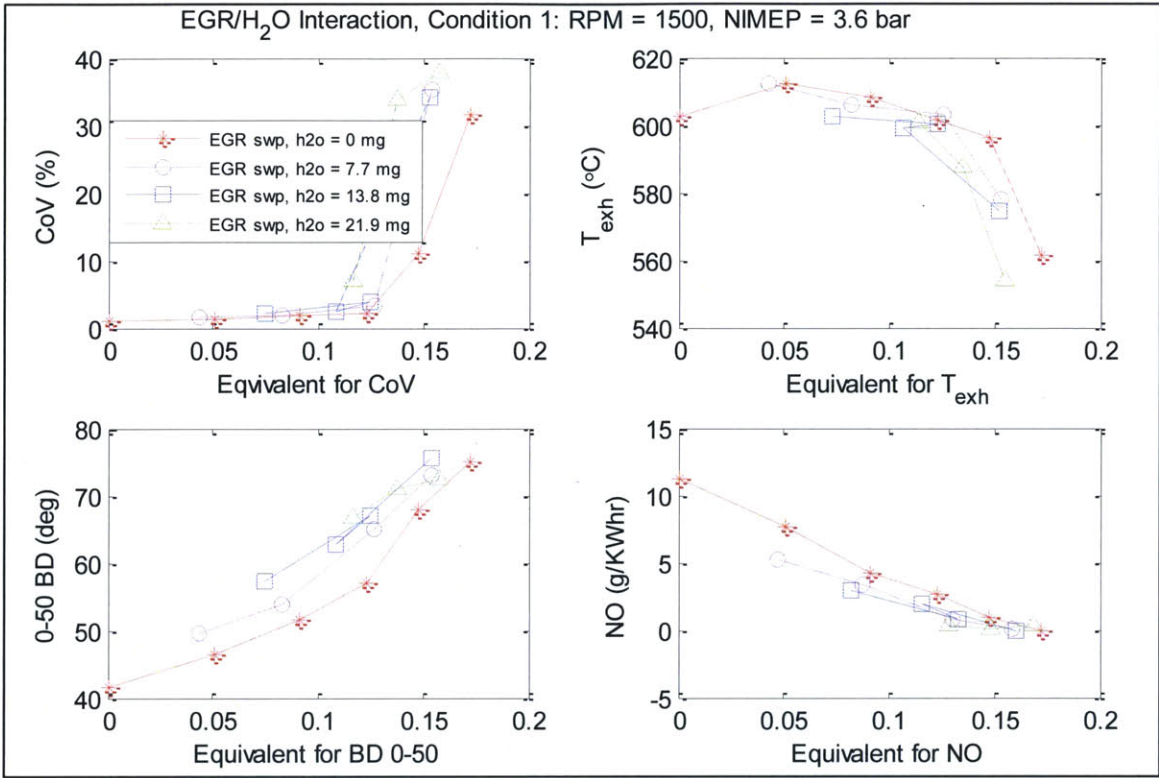
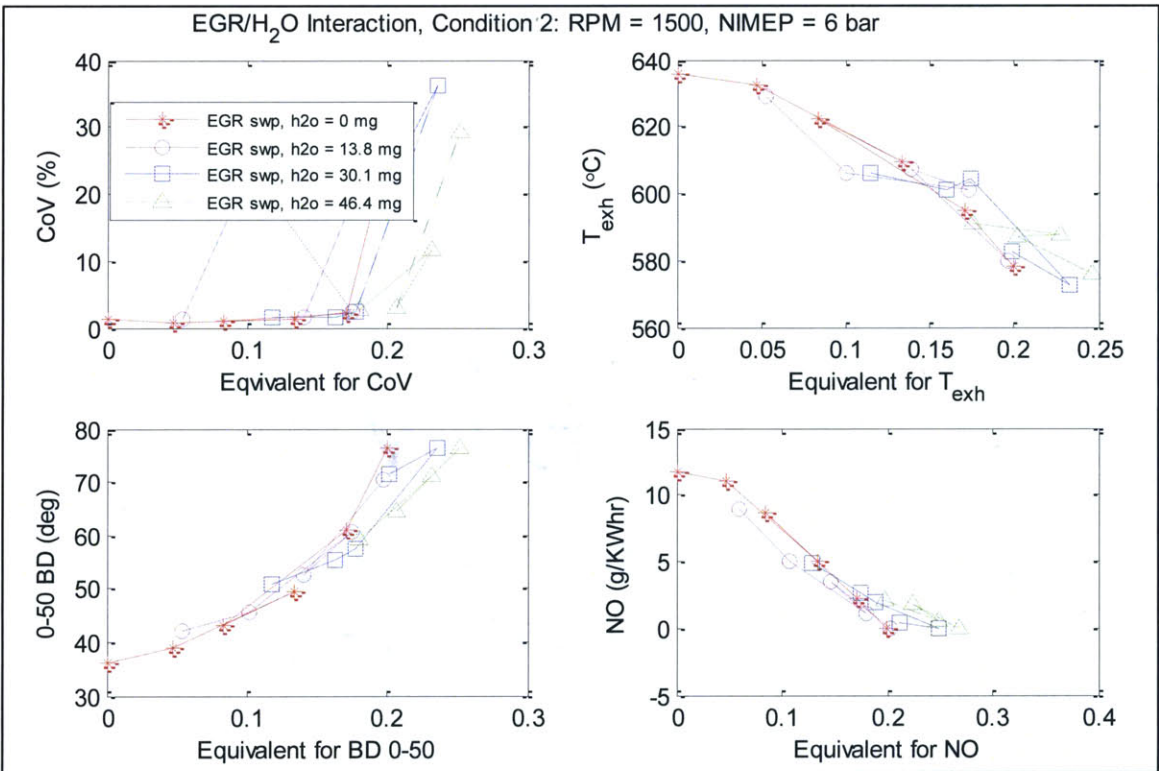


Figure 45: EGR – Lean Interaction, Condition 3



**Figure 46: EGR – H<sub>2</sub>O Interaction, Condition 1**



**Figure 47: EGR – H<sub>2</sub>O Interaction, Condition 2**

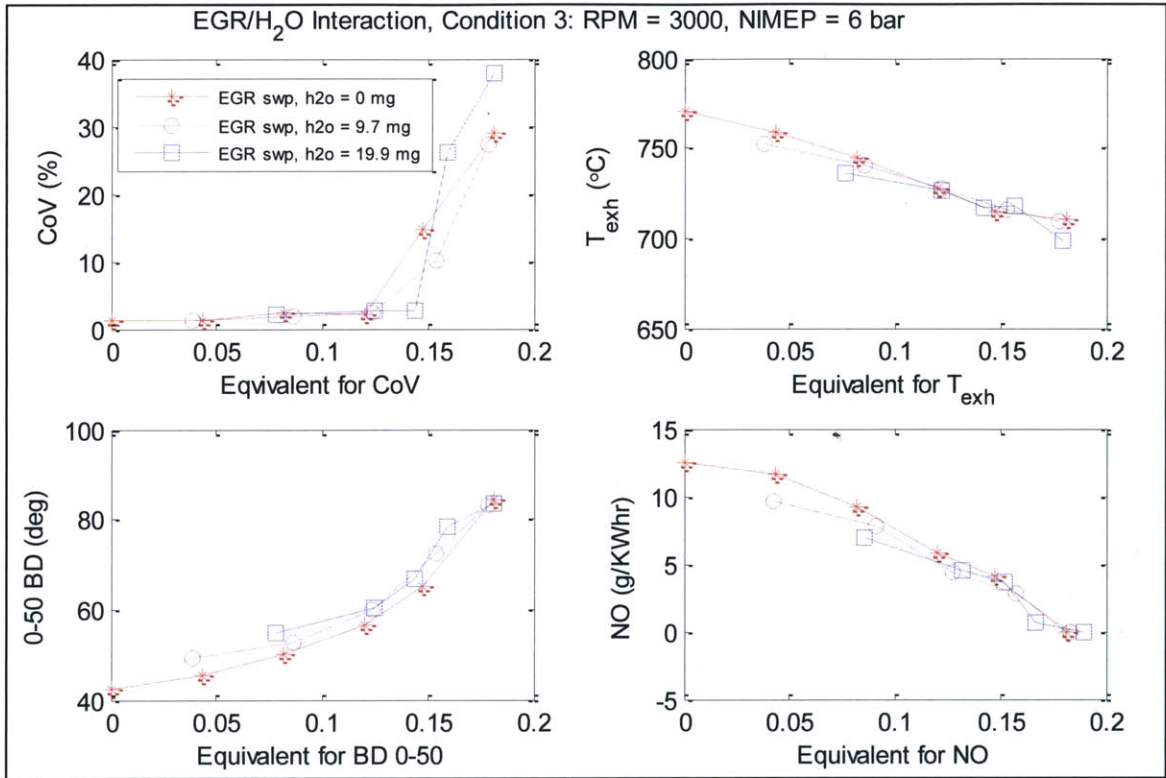


**Figure 48: EGR – H<sub>2</sub>O Interaction, Condition 3**